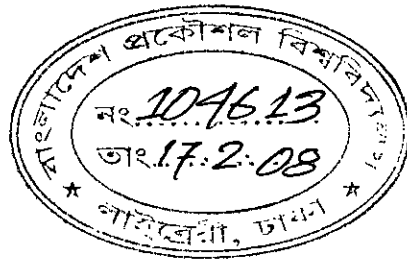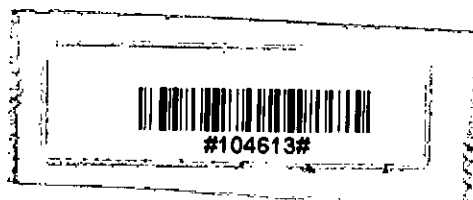# Analysis of Crosstalk Due to Unidirectional and Bidirectional Optical Cross-Connects in a WDM Network

A thesis submitted to the Department of Electrical and Electronic Engineering of Bangladesh University of Engineering and Technology in partial fulfillment of the requirement for the degree of

MASTER OF SCIENCE IN ELECTRICAL AND ELECTRONIC ENGINEERING

by
Mohammad Jalal Uddin

DEPARTMENT OF ELECTRICAL AND ELECTRONIC ENGINEERING
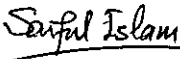BANGLADESH UNIVERSITY OF ENGINEERING AND TECHNOLOGY
2008

APPROVAL CERTIFICATE

The thesis titled **"Analysis of Crosstalk Due to Unidirectional and Bidirectional Optical Cross-Connects in a WDM Network"** submitted by Mohammad Jalal Uddin, Roll No.: 040406269P, Session: April, 2004 has been accepted as satisfactory in partial fulfillment of the requirement for the degree of Master of Science in Electrical and Electronic Engineering on February 06, 2008.

BOARD OF EXAMINERS

1. _____

   Prof. Dr. Satya Prasad Majumder   Chairman
   Professor and Head   (Supervisor & Ex-Officio member)
   Department of Electrical and Electronic Engineering
   Buet, Dhaka - 1000, Bangladesh.

2. _____

   Prof. Dr. Saiful Islam   Member
   Professor
   Department of Electrical and Electronic Engineering
   Buet, Dhaka - 1000, Bangladesh.

3. _____

   Dr. Md. Shah Alam   Member
   Associate Professor
   Department of Electrical and Electronic Engineering
   Buet, Dhaka - 1000, Bangladesh.

4. _____

   Prof. Dr. Farruk Ahmed   Member
   Professor   (External)
   Department of Computer Science and Engineering
   North South University, Dhaka, Bangladesh.

Declaration

It is hereby declared that this thesis or any part of it has not been submitted elsewhere for the award of any degree or diploma.

Signature of the candidate

(Mohammad Jalal Uddin)

Dedication

To My Parents

Contents

List of Figures

List of Tables

List of Symbols

σ_{th}^2	thermal noise of the optical receiver
σ_{intra}^2	noise power due to intra-band or in-band crosstalk
σ_{inter}^2	noise power due to inter-band crosstalk
σ_{bs}^2	noise power due to backscattering induced crosstalk
σ_1^2	variance of output of the receiver for binary '1'
σ_0^2	variance of output of the receiver for binary '0'
k	boltzman constant
T	room temperature in degree kelvin
λ	wavelength
N	number of channels or number of input ports
M	number of wavelengths per channel
R_c	component crosstalk
R_{bs}	equivalent reflectivity of backscattering
$\Delta\lambda$	Channel separation
P_T	Received Power
n_{eff}	effective refractive index
λ_{Bragg}	Bragg wavelength
κ	coupling coefficient
η	quantum efficiency
G	gain of optical amplifier
B_e	electrical bandwidth of the receiver
B_o	optical bandwidth of the receiver
σ_{shot}^2	shot noise of the optical receiver
P_{ASE}	noise power of amplified spontaneous emission
h	Planck's constant
σ_{s-ASE}^2	signal-ASE beat noise
$\sigma_{ASE-ASE}^2$	ASE-ASE beat noise

List of Abbreviations

WDM	Wavelength Division Multiplexing
EDFA	Erbium-Doped Fiber Amplifier
OXC	Optical Cross-Connect
OPXC	Optical Path Cross-Connect
FBG	Fiber Bragg Grating
AWG	Arrayed Waveguide Grating
BOXC	Bidirection Optical Cross-Connect
BWRN	Bidirectional WDM Ring Network
RIN	Relative Intesity Noise
BER	Bit Error Rate
PP	Power Penalty
LD	Laser Diode
MZI	Mach-Zehnder Interferometer
FPF	Fabry Perot Filter
TFF	Thin Film Filter
FPR	Free Propagation Region
FWHM	Full Width Half Maximum
OA	Optical Amplifier
SOA	Semiconductor Optical Amplifier
OC	Optical Circulator
ASE	Amplified Spontaneous Emission
OLT	Optical Line Terminals
OADM	Optical Add/Drop Multiplexer
SONET	Synchronous Optical Network
IP	Internet Protocol
O/E/O	Optical to Electrical to Optical
O/E	Optical to Electrical
OSC	Optical Supervisory Channel
MAN	Metropolitan Area Network

Acknowledgement

This is my immense pleasure to express my sincere and profound gratitude to my supervisor Prof. Dr. Satya Prasad Majumder, Professor, Department of Electrical and Electronic Engineering (EEE), Bangladesh University of Engineering and Technology (BUET), Dhaka, for providing me the opportunity to conduct graduate research in recent research area of optical fiber communication. I wish to convey my heartfelt thank to him for his continuous guidance, kind help and wholehearted encouragement during the course of the work, without which this work would never be possible.

I want to thank my wife, Mrs. Tanzina Jalal for her assistance during the writing of this dissertation and her continuous support during my work. I would like to express my gratitude to my parents and my in law parents for their encouragement and love during my course of work.

I also want to thank Prof. Dr. Saiful Islam, Prof. Dr. Farruk Ahmed and Dr. Md. Shah Alam for being the part of my defense committee.

Finally, I am grateful to Almighty Allah for enabling me to complete the thesis.

Abstract

A theoretical analysis is presented to find the impact of crosstalk due to optical cross-connects (OXCs) in a WDM network. An $N \times N$ AWG based OXC is first considered with one wavelength per channel. Thereafter, a mux/demux based OXC with N number of channels and M number of wavelengths per channel is investigated. The analytical expressions of in-band and out-band(inter-band) crosstalks due to these OXCs are developed. The expression for BER is derived considering the effect of in-band and inter-band crosstalk together for unidirectional operation of an OXC in a WDM system. Analysis is also extended to bidirectional OXC in a WDM network considering the impact of crosstalk and backscattering. Performance results are evaluated numerically considering M-channel WDM system with $N \times N$ OXC operating at a bit rate of 10 Gb/s with several system parameters. Performance degradation in terms of BER and power penalty due to OXC induced crosstalk is evaluated and optimum system design parameters are determined for operation of a bit rate of 10 Gb/s and BER of 10^{-9}. The results will find application in designing a multiwavelength WDM optical transport network.
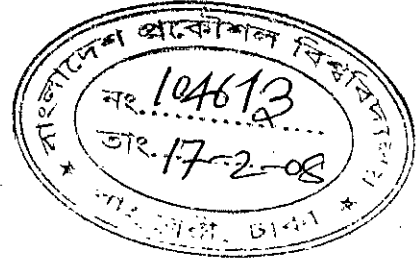
Chapter 1

Introduction

The growth of telecommunication is expected to continue, spurred on by several factors, including the globalization of world economy, the strong dependance of modern industry and society on telecommunications and information systems, and the public demand for access to telecommunication. Indeed, the continuous increasing demand for high information capacity systems assures the presence of fiber optical communication systems in the information era.

Although, optical communication, for instance, by fires, smoke, semaphore flags and optical telegraphs, has been used since a long time ago for information transmission, it is in the first half of the 19th century with the invention of the telegraph, the introduction of telephony and later television that the infrastructure of telecommunication networks are started to emerge. Soon higher and higher transmission capacities were demanded from this telecommunication networks. At first, pair cables were replaced for coaxial cables for providing a higher capacity. Others medium of transmission were introduced as microwave links and satellite communications.

The area of optical fiber communication has shown a very fast technical development. This is mainly due to a combination of progress in semiconductor, optical waveguide and photonic integration technology. Today, through the world, telecommunication operators use optical fiber for transmission of information in long distant systems, undersea systems, metropolitan area networks, and in access

and distribution networks, among others.

1.1   Brief Historical Review

In 1966, Kao, Hockman and Werts suggested that if it would be possible to produce a glass fiber of sufficiently low attenuation, optical fibers would be alternate to coaxial cables for information transmission. The idea is based on the fact that light can be confined and propagate in an optical fiber by total internal reflection at certain angles in a guiding media with different refractive index n_1 and n_2 as shown in Figure 1.1.
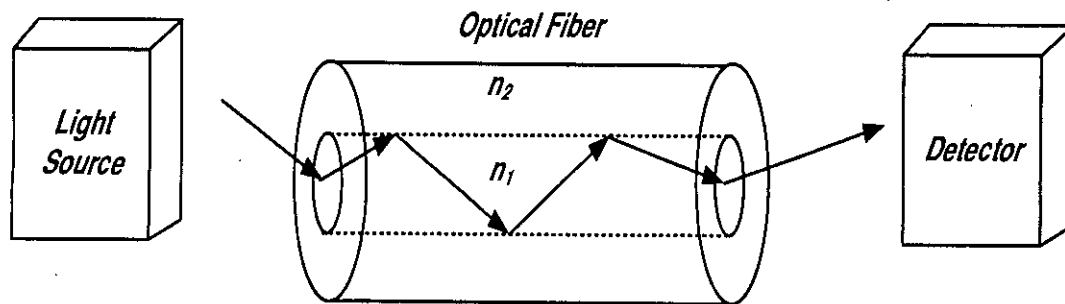
Figure 1.1: Principle of optical fiber communication.

Improvement in the quality of the optical fiber made possible the introduction of first generation of optical fiber communication in 1970's. These systems used laser sources operating at the wavelength region of 800 nm. The further development has been to operate at 1300 nm and 1550 nm wavelengths due to the superior silica fiber dispersion and attenuation properties; the so called second and third generation of optical communication system. The development of low loss fiber of approximately 0.2 dB/km and single mode laser sources has made possible the deployment of long distance fiber optic communication system.

An event of major impact on the development of fiber optical communication is the advent of the optical fiber amplifier known as EDFA(erbium doped fiber amplifier) in 1987. The introduction of EDFA, replacing the opto-electrical regeneration, revolutionized the field of optical fiber communication, mainly because of

their potential to enhance the transmission length, transparency to modulation format, polarization insensitivity, low noise and crosstalk and an ease of splicing to the fiber transmission system. The fourth generation of fiber optical communication systems uses wavelength division multiplexing(WDM) to increase the information capacity and EDFAs to enhance the transmission length. In 1996, WDM point-to-point systems were commercially introduced and they have become the choice of preference to expand and upgrade the transmission capacity of optical fiber transmission system. The next generations of communication systems are expected to be based on advance transmission techniques like optical soliton transmission, novel modulation schemes, and intelligent nodes. Research on the coming generation of optical system is in progress both in industry and university research centers.

1.2 Brief Introduction of WDM Systems

With the unprecedented growth in telecommunication and data traffic, and the urgent demand for diverse services, the capacity increase of transmission system is needed. Wavelength-division multiplexing (WDM) is one promising approach that can be used to exploit the huge bandwidth of optical fiber to meet this demand. WDM is essentially the same as frequency division multiplexing, which has been used in radio communication for more than a century. WDM can be defined in which multiple optical carriers(which are not in phase with each other) at different wavelengths are modulated by using independent electrical bit streams and multiplexed together and are then transmitted over the same fiber. The optical signal at the receiver is demultiplexed back into separate channels. Thus, by allowing multiple WDM channels to coexist on a single fiber, we can tap into the huge fiber bandwidth.

The first WDM systems only combined two signals, one channel is at 1.33 μm and the another is at 1.55 μm. Modern systems can handle up to 160 signals and can thus expand a basic 10 Gbits/s fiber system to a theoretical total capacity of over 1.6 Tbits/s over a single fiber pair. A simple WDM system is shown in Figure 1.2.
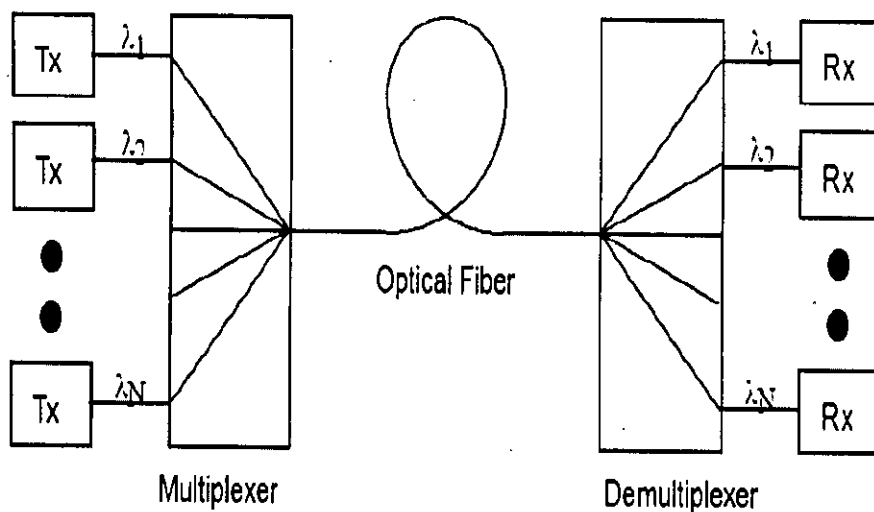
Figure 1.2: A simple WDM system. Multiplexer combines N number of wavelengths together from N number of transmitters. Optical fiber is used to carry this multiplexed signal. Demultiplexer separates these N wavelengths and sends them to N receivers.

1.3 All-Optical Network

All-optical networks have emerged as a solution to keep up with the always increasing throughput demand. In todays transport networks, data are transmitted over optical fibers and optical-electro-optical conversion is needed at the nodes to perform routing. These networks can achieve a throughput of up to several hundreds of Gbits/s using Wavelength Division Multiplexed (WDM) channels. Yet optical fibers have a potential capacity of several tens of Tbits/s per channel. Electronic switches are not able to sustain such transmission rates and have become complex and costly, making it highly desirable to replace them with all-optical switches where no electric conversion is needed at all. Deploying such all-optical networks is promising but also challenging and novel issues have to be anticipated. In this dissertation, we study one of these issues, impairment by optical leaks, called node crosstalk, which takes place in switches.

All-optical switches, or optical cross-connects (OXCs), remove the electrical conversion step in switching hardware. In addition to the gain in network data rate, all-optical switches are expected to become simpler to implement and therefore cheaper than their electrical counterparts. Moreover, all-optical switches allow for improved data rate flexibility in networks. All-optical switches have been the subject of much research in the recent years and some are already commercially available. The function of an all-optical switch is to transmit an incoming signal arriving along a certain optical fiber on a certain wavelength to a different optical fiber. Although several architectures have been proposed [2] and [3], all-optical switches contain the same functional elements: demultiplexers, a switching fabric, optional wavelength converters, and multiplexers. In our work, we do not consider wavelength conversion nor optical regenerators.

1.4 Literature Review

Fiber optic communications have provided us with high-speed communications with enormous bandwidth potential. WDM enables the utilization of a significant portion of the available fiber bandwidth by allowing many independent signals to be transmitted simultaneously on one fiber, with each signal being on a different wavelength. OXCs are the essential element of WDM systems and crosstalk that arises due to the leak in OXC is our main focus of this study. Hill *et al.* [1] presented an approach to the realization of a future broad-band flexible transport network employing an optical network layer. The design methodology for a network demonstrator is presented and a description of the subsystem and component technology developments is described.

Iannone *et al.* [2] presented different optical cross-connect architectures, based either on space division or wavelength division switching. A comparative investigation is accomplished considering three issues of primary importance: cross-connect modularity, complexity, and transmission performance. In particular, the transmission performance of a generic path through the network is evaluated by upgrading a previously published analytical model, to more accurately take into account the in-band crosstalk arising in the cross-connect.

Optical path technologies will play a key role in the development of the platform on which the future bandwidth abundant B-ISDN should be created. Okamoto *et al.* [3] explored the optical path cross-connect (OPXC) node architectures that are essential components of the optical path network.

Zhou *et al.* [4] studied optical crosstalk in multi wavelength optical cross-connect networks. Two crosstalk mechanisms, inter-band and intra-band crosstalk, caused by non ideal wavelength demultiplexing and space switching are identified and their nature and accumulation behavior are studied in detail.

Tim *et al.* [5] presented the results of crosstalk analysis of four optical wavelength division multiplexed (WDM) cross-connect (OXC) topologies. An optimal set of parameters is determined to reduce the total crosstalk. The total crosstalk as a function of the number of cascaded OXCs is compared for the four topologies.

Takahashi *et al.* [6] presented the impact of crosstalk in an arrayed-waveguide $N \times N$ wavelength multiplexer. It is shown that in such systems, multiple crosstalk light which has the same wavelength as the signal results in signal-crosstalk beat noise. They confirmed that the noise is Gaussian and obtained the relation between crosstalk and power penalty.

Dods *et al.* [7] and [9] examined the effects of coherent and incoherent homodyne crosstalk in WDM ring and bus networks using reconfigurable optical add/drop multiplexers (OADMs). They showed that that the coherent and incoherent crosstalk together lead to a range of possible power penalties.

Keang-Po *et al.* [8] presented an exact analytical probability density function and a closed form BER formula for the WDM networks with homodyne crosstalk from a single dominant channel.

Shen *et al.* [10] studied the impact of coherent and incoherent crosstalk on an optical signal passing through optical cross-connect nodes (OXCs) in WDM optical networks. They have shown that coherent crosstalk can either cause the

noise or not depending on the optical delay difference and the bit duration of the signal.

Kim *et al.* [11] demonstrated a cost-effective bidirectional WDM self-healing ring network using a novel bidirectional add/drop amplifier module. The maximum power penalty incurred in this network for bidirectional transmission and add/drop multiplexing of WDM signals was measured to be less than 0.5 dB at an error rate of 10^{-9}.

Park *et al.* [13] proposed a multiwavelength bidirectional optical crossconnect (BOXC) structure based on fiber Bragg gratings (FBGs) and polarization beam splitters (PBSs). A 2 × 2 BOXC system is implemented using four pairs of short period gratings and two PBSs, in order to experimentally evaluate the performance of the proposed BOXC system.

As the single fiber bidirectional ring network develops, independently switchable bidirectional optical cross connects (IS-BOXCs) that switch each bidirectional optical signal, both independently and simultaneously will be needed. Kim *et al.* [14] proposed new structures of IS-BOXCs using two different unidirectional optical cross connects. The proposed IS-BOXCs sufficiently suppress the relative intensity noise caused by Rayleigh backscattering and optical reflection.

Kim *et al.* [15] proposed a BOXC using a single arrayed waveguide grating(AWG) router and tunable FBGs for multi wavelength BWRNs. Two types of structures in fold-back and loop-back configurations have been considered and their feasibility has been demonstrated experimentally. The performances of two proposed structures have been investigated and compared in terms of crosstalk characteristics and backscattering suppression capability.

Zhong *et al.* [16] proposed a new bidirectional optical cross connect (BOXC) using fiber Bragg gratings (FBGs) and optical circulators for bidirectional wavelength division multiplexing ring networks(BWRNs). Dynamic and independent wavelength routing is achieved by employing cascaded tunable FBGs.

1.5   Background of this Study

Wavelength division multiplexed (WDM) optical networks are attracting more
and more attention because of their ability to provide increased capacity and flex-
ibility [1]. Optical cross-connect (OXC) is an essential network element in a
WDM optical network [2]. A number of OXC architectures have been proposed
in [2] and [3], each of which have its own unique features, strengths, and limi-
tations. Imperfections of the optical components used in these architectures give
rise to optical crosstalk [4], [5]. Crosstalk is classified as homodyne (intra-band
or in-band) and heterodyne (inter-band) crosstalk. Homodyne crosstalk has the
same wavelength as the signal and degrades the transmission performance seri-
ously [6]− [10]. Because of the identical wavelength, this crosstalk is difficult
to be eliminated by filtering and the crosstalk beats with the signal and gener-
ates beat noise components at the receiver output [6]. Homodyne crosstalk can
be divided into coherent crosstalk, whose phase correlated with the signal con-
sidered and incoherent crosstalk, whose phase is not correlated with the signal.
In recent years, the importance of high capacity WDM networks has been more
emphasized. Network providers face the need to satisfy user demand both for
significantly higher network capacity and for improved reliability. Bidirectional
WDM ring networks have received a great attention for their cost effective of en-
hancing capacities and possibility of self-healing characteristics [11]. Bidirectional
optical cross connects (BOXCs) are key switching elements in bidirectional WDM
ring networks (BWRNs), which could selectively interchange wavelength channels
among the BWRNs in both directions. Several types of BOXCs are reported in
[12]− [16]. Study of the crosstalk due to BOXCs and its effect on a WDM network
is yet to be reported.

1.6 Objectives

In this research, performance degradation in all-optical transport networks caused by node crosstalk originating from leaks in OXCs is studied. The six objectives of this research work are:

1. To make detail analysis of homodyne (intra-bnad or in-band) crosstalk in unidirectional OXCs based on arrayed waveguide grating (AWG).

2. To develop an analytical expression for the heterodyne (inte-rband) crosstalk.

3. To evaluate the BER and power penalty due to in-band and iter-band crosstalk in a WDM network.

4. To carry out detail analysis of crosstalk due to AWG and FBG based bi-directional OXCs and the analysis of backscattering in bi-directional OXCs.

5. To evaluate the BER in a WDM network considering the crosstalk and backscattering due to bi-directional OXCs.

6. To determine the power penalty due to crosstalk and backscattering in bi-directional OXCs and to find the optical system parameters at a given BER.

1.7 Research Methodology

To achieve the objectives described in section 1.6, we have done our analysis in several steps. At first, to evaluate the impact of homodyne crosstalk, analytical expression for the relative intensity noise (RIN) due to homodyne crosstalk has been developed. Then, an analytical expression for the heterodyne crosstalk has also been developed. The expression for BER of a WDM network considering the effects of both homodyne and heterodyne crosstalk has been derived and the BER performance results are evaluated in terms of received power, number of fibers, number of wavelengths and different component crosstalk. Power penalty due to crosstalk at a given BER is evaluated from the results obtained above.

To analyze the BOXC, the crosstalk due to the backscattering in a BOXC has been considered. The expression of BER of a WDM system is also derived considering both the component crosstalk and backscattering induced crosstalk. The BER performance results and power penalty is evaluated considering all homodyne, heterodyne and backscattering induced crosstalk.

1.8   Organization of the Thesis

Chapter 2 gives a overview of WDM system. The operation principle, basic characteristics of different WDM components and network elements are briefly discussed in this chapter.

Chapter 3 starts with the classification of different crosstalk present in OXC. The theoretical analysis and the analytical expression of different crosstalk is given thereafter. Finally the effect of crosstalk in the BER performance is presented analytically.

Chapter 4 presents the results and discussion. The BER performance and the power penalty is observed in presence of different crosstalk present in the OXCs.

Chapter 5 presents the conclusive remarks of this thesis along with the limitation and the scope of future work.

Chapter 2

Overview and Modeling of WDM Systems

In this chapter, a brief introduction of WDM components and network elements is given. At the end of this chapter, WDM system models of our current study are presented for unidirectional and bidirectional optical fiber communication.

2.1 WDM Components

WDM system consists of the following components:

1. Transmitters

2. Couplers

3. Muliplexers/Demultiplexers and Filters

4. Optical fiber

5. Optical amplifiers

6. Circulators

7. Wavelength converters or transponders

8. Optical switches

9. Receivers

2.1.1 Transmitters

A fiber optic transmitter converts electrical signals into optical signals and launches the optical signals into an optical fiber. Light emitted by an optical source is launched, or coupled, into an optical fiber for transmission. Semiconductor optical sources suitable for fiber optic systems range from inexpensive light-emitting diodes (LEDs) to more expensive semiconductor lasers. Semiconductor LEDs and laser diodes (LDs) are the principal light sources used in fiber optics.

The development of efficient semiconductor optical sources, along with low-loss optical fibers, led to substantial improvements in fiber optic communications. Semiconductor optical sources should have the following physical characteristics and performance properties necessary for successful implementations of fiber optic systems.

1. Be compatible in size to low-loss optical fibers by having a small light-emitting area capable of launching light into fiber.

2. Launch sufficient optical power into the optical fiber to overcome fiber attenuation and connection losses allowing for signal detection at the receiver.

3. Emit light at wavelengths that minimize optical fiber loss and dispersion. Optical sources should have a narrow spectral width to minimize dispersion.

4. Maintain stable operation in changing environmental conditions (such as temperature).

5. Allow for direct modulation of optical output power.

6. Cost less and be more reliable than electrical devices, permitting fiber optic communication systems to compete with conventional systems.

Fiber optic communication systems operate in the 850 nm, the 1300 nm, and the 1550 nm wavelength windows. Semiconductor sources are designed to operate at wavelengths that minimize optical fiber absorption and to maximize system bandwidth. By designing an optical source to operate at specific wavelengths, absorption from impurities in the optical fiber, such as hydroxyl ions (OH-), can

be minimized. Maximizing system bandwidth involves designing optical fibers and sources that minimize chromatic and intermodal dispersion at the intended operational wavelength.

2.1.2 Couplers

An optical coupler is a passive device for branching or coupling an optical signal. There are mainly two types of couplers:

1. Directional coupler

2. Star coupler

Directional Coupler

A directional coupler is used to combine and split signals into optical networks. A 2×2 coupler consists of two input ports and two output ports as shown in Figure 2.1. Optical couplers are made by fusing and tapering two fibres together so that the cores are close enough to each other for optical coupling to occur. A 2×2
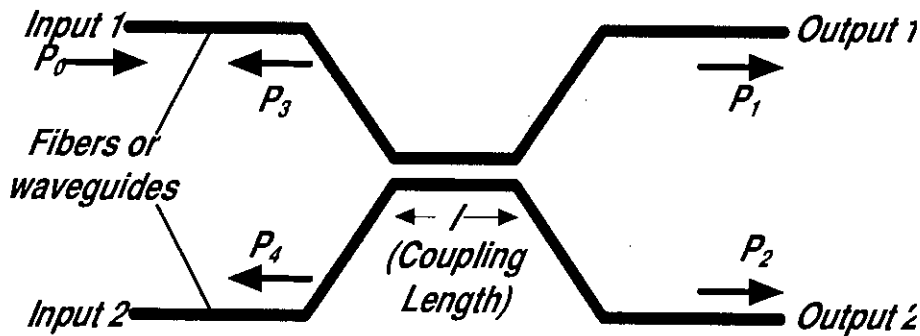
Figure 2.1: A directional coupler.

coupler as shown in Figure 2.1, takes a fraction α of the power from input 1, P_0 and places it on output 1, P_1 and the remaining portion $1 - \alpha$ on output 2, P_2. We call α the coupling ratio.

$$P_1 = \alpha P_0$$

$$P_2 = (1 - \alpha)P_0$$

P_3 and P_4 are extremely low level signal resulting from back reflection and scattering due to bending and packaging of the device. The coupling length l can be adjusted to make $\alpha = 0.5$. In this case, power is equally distributed in two outputs. This type of coupler is called a 3-dB coupler.

The electric fields, E_{o1} and E_{o2}, at the outputs of a directional coupler may be expressed in terms of the electric fields at the inputs E_{i1} and E_{i2} as follows [18]:

$$\begin{pmatrix} E_{o1}(f) \\ E_{o2}(f) \end{pmatrix} = e^{-i\beta l} \begin{pmatrix} \cos(kl) & i\sin(kl) \\ i\sin(kl) & \cos(kl) \end{pmatrix} \begin{pmatrix} E_{i1}(f) \\ E_{i2}(f) \end{pmatrix} \tag{2.1}$$

here, l is the coupling length and β is the propagation constant in each of the two waveguide of the directional coupler.

Though the directional coupler is a two-input, two-output device, it is often used with only active input, say input 1. In this case, the power transfer function of the directional coupler is given by [18],

$$\begin{pmatrix} T_{11}(f) \\ T_{12}(f) \end{pmatrix} = \begin{pmatrix} \cos^2(kl) \\ \sin^2(kl) \end{pmatrix} \tag{2.2}$$

Here, $T_{ij}(f)$ represents the power transfer function from input i to output j and is defined by $T_{ij}(f) = |E_{oj}|^2/|E_{ii}|^2$. Equation 2.2 can be derived from equation 2.1 by setting $E_{i2} = 0$.

To achieve the conservation of energy of input and output electric field, it can be shown that for a 3-dB coupler, though the electric field at the output have the same magnitude, they have a relative phase shift of $\pi/2$. This relative phase shift plays an important role in the design of device such that MZI as discussed in section 2.1.3.

Star Coupler

The principal role of star coupler is to combine the power from N inputs and divide them equally among M output ports. The number of input and output ports for

star coupler is greater than four. Techniques for creating star coupler include fused fibers, grating, micro-optic technologies, and integrated-optics schemes. Figure 2.2 shows a 6×6 fused-fiber star coupler.
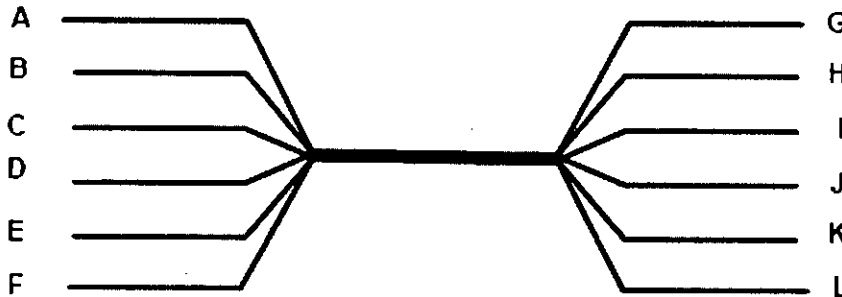
Figure 2.2: A Generic 6×6 star coupler.

An alternative is to construct star couplers by cascading 3-dB couplers. Figure 2.3 shows an example for an 8×8 device formed by using twelve 2×2 couplers. This device could be made from either fused-fiber or integrated-optic components. As can be seen from this figure, a fraction $1/N$ of the launched power from each input port appears at all output ports. A limitation to the flexibility and modularity of this technique is that N is a multiple of 2; that is, $N = 2^n$ with the integer $n \geq 1$. The consequence is that if an extra node needs to be added to a fully connected $n \times N$ network, the $n \times N$ star needs to be replaced by a $2N \times 2N$ star, thereby leaving $2(N - 1)$ ports being unused.

2.1.3 Multiplexers/Demultiplexers and Filters

Mach-Zehnder Interferometers

A Mach-Zehnder interferometer(MZI) is an interferometric device that makes use of two interfering paths of two different lengths to resolve different wavelengths. Devices constructed on this principle have been available for some decades. Today, MZI is typically constructed in integrated optics and consists of two 3-dB couplers interconnected through two paths of different lengths, as shown in Figure 2.4(a).
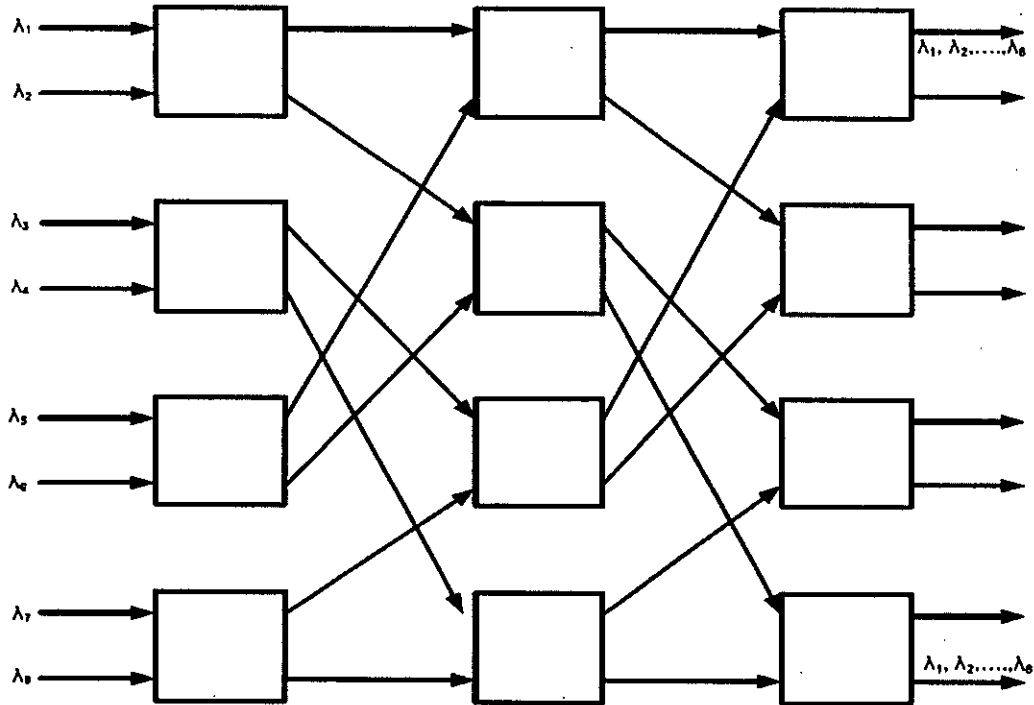
Figure 2.3: Example of an 8 × 8 star coupler formed by interconnecting twelve 2 × 2 couplers.

Even though there are better technologies for making narrow band filters, MZIs are still useful in realizing wide band filters. Very good crosstalk performance can be achieved if the wavelengths are spaced such that the undesired wavelengths occur at, or close to the null of the power transfer function.

MZIs are useful as both filters and multiplexers/demultiplexers. They can also be used as a tunable filters, where the tuning is achieved by varying the temperature of one of the arms of the device.

Let us consider the operation of MZI as demultiplexer and input 1 as shown in Figure 2.4 has a signal. After the first directional coupler, the input signal power is divided equally between the two arms, but the signal in one arm has a phase shift of $\pi/2$ with respect to the other as discussed in section 2.1.2. From equation 2.1, it can be understood that the signal in the lower arm will lag by $\pi/2$. Since, there is a length difference of ΔL between the two arms, there is a further phase
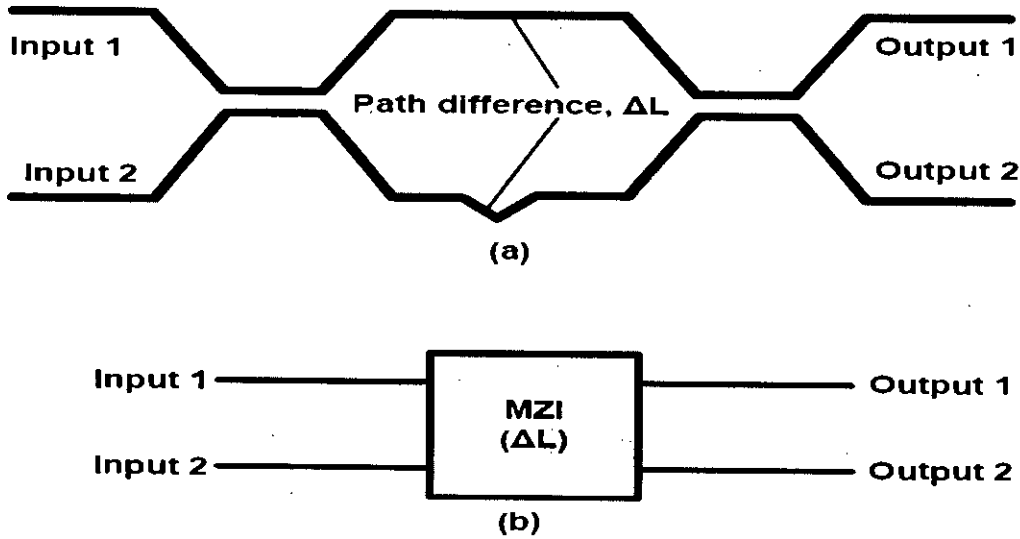
Figure 2.4: (a)An MZI constructed by two 3-dB couplers; (b)A block diagram representing the MZI in (a).

lag of $\beta\Delta L$, introduced in the signal in the lower arm. In the second directional coupler, the signal from the lower arm undergoes another phase delay of $\pi/2$ in going to the first output relative to the signal from the upper arm. Thus the total relative phase difference at the first or upper output between the two signals is $\pi/2 + \beta\Delta L + \pi/2 = \pi + \beta\Delta L$. At the output of the directional coupler, in going to the second output, the signal from the upper arm lags the signal from the lower arm by $\pi/2$. Thus the total relative phase difference at the second or lower output between the two signals is $\pi/2 + \beta\Delta L - \pi/2 = \beta\Delta L$.

If $\beta\Delta L = k\pi$ and k is odd, the signals at the first output add in phase, whereas the signal at the lower output add with opposite phases and thus cancel each other. Thus the wavelengths passed from the first input to the first output are those wavelengths for which $\beta\Delta L = k\pi$ and k is odd. The wavelengths passed from the first input to the second output are those wavelengths for which $\beta\Delta = k\pi$ and k is even. This could be easily deduced from the transfer function of the MZI as given by equation 2.3.

Assuming that the difference between these path lengths is ΔL and that only one input, say, input 1 is active, it can be shown that the power transfer function of the MZI is given by [18],

$$
\begin{pmatrix} T_{11}(f) \\ T_{12}(f) \end{pmatrix} = \begin{pmatrix} \sin^2(\beta \Delta L/2) \\ \cos^2(\beta \Delta L/2) \end{pmatrix}
\tag{2.3}
$$

Thus the difference between two arms, ΔL, is the key parameter characterizing the transfer function of the MZI. Since the device is reciprocal, it follows from the principle of electromagnetics that if the inputs and outputs are interchanged, it will act as a 2×1 multiplexer.

A typical 8 channel multiplexer/demultiplexer is shown in Figure 2.5. The number of stages required for 8 channel mux/demux is $\log_2 8 = 3$.
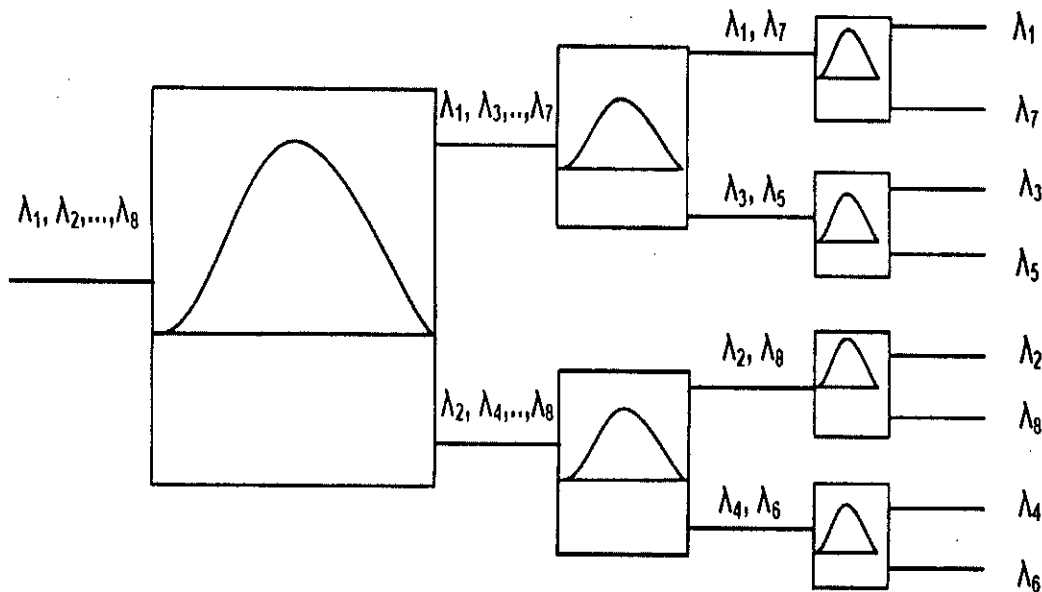
Figure 2.5: An 8 channel WDM mux/demux using MZIs. After the first stage odd numbered wavelengths interfere additively at the upper output and the even numbered wavelengths interfere additively at the lower output. By using the same principle other wavelengths are being separated by the rest of the MZIs.

Fabry-Perot Filtes

A Fabry-Perot filter consists of the cavity formed by two highly reflective mirrors placed parallel to each other, as shown in Figure 2.6. This filter is also known
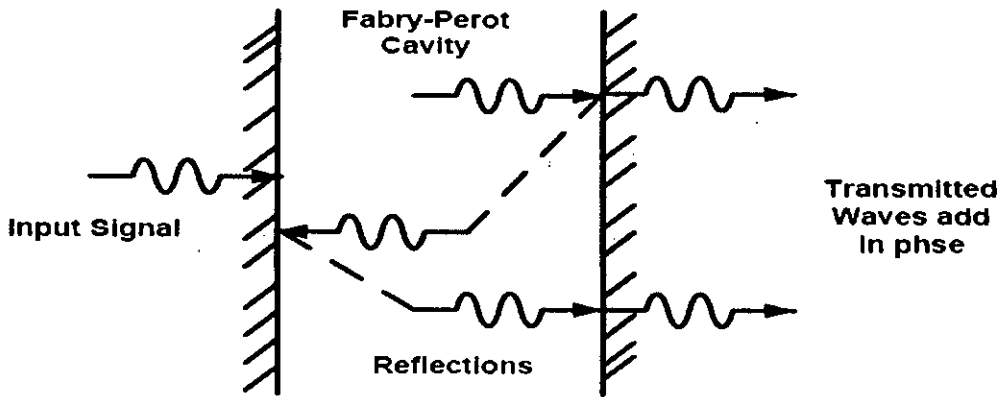
Figure 2.6: Principle of operation of Fabry-Perot filter.

as Fabry-Perot interferometer or elaton. The input light beam to the filter enters the first mirror at right angles to its surface. The output of the filter is the light beam leaving the second mirror.

The principle of operation of the device is shown in Figure 2.6. The input signal is incident on the left side of the cavity. After one pass through the cavity, as shown in Figure 2.6, a part of the light leaves the cavity through the right facet and a part is reflected. A part of the reflected wave is again reflected by the left facet to the right facet. For those wavelengths, for which the cavity length is an integral multiple of half the wavelength in the cavity, so that a round trip through the cavity is an integral multiple of wavelength, all the light waves transmitted through the right facet add in phase. Such wavelengths are called the resonant wavelengths of the cavity.

The power transfer function of a filter is the fraction of input light power that is transmitted by the filter as a function of optical frequency f, or wavelength. For

the Fabry-Perot filter, this function is given by [18],

$$T_{FP}(f) = \frac{\left(1 - \frac{A}{A-R}\right)^2}{\left(1 + \left(\frac{2\sqrt{R}}{1-R}\sin(2\pi f\tau)\right)^2\right)} \qquad (2.4)$$

Here **A** denotes the absorption loss of each mirror, which is the fraction of the incident light that is absorbed by the mirror. **R** denotes the reflectivity of the each mirror, which is the fraction of the incident light that is reflected by the mirror.

A Fabry-Perot filter can be tuned to select different wavelengths in one or several ways. The simplest approach is to change cavity length. The same effect can be achieved by varying the refractive index within the cavity.

Thin Film Filter

A thin film filter(TFF) is a Fabry-Perot interferometer or elaton, in which the mirrors surrounding the cavity are realized by using multiple reflective dielectric thin-film layer. This device acts as bandpass filter, passing through a particular wavelength and reflecting all the other wavelengths. The wavelengths that is passed through is determined by the cavity length. In order to obtain a multiplexer or a demultiplexer, a number of these filters can be cascaded as shown in Figure 2.7. Each filter passes a different wavelength and reflects all the others. When used as a demultiplexer, the first filter in the cascade passes one wavelength and reflects all the others onto the second filter. The second filter passes another one wavelength and reflects the remaining ones, and so on.

This device has many attractive features for system application. It is possible to have very flat top and very sharp skirts. The device is extremely stable with temperature variation, has loss, and is insensitive to the polarization of the signal.

Arrayed Waveguide Grating

The Arrayed Waveguide Grating (AWG) plays a crucial role in the realisation of modern optical networks. Arrayed Waveguide Gratings (AWGs) are optical
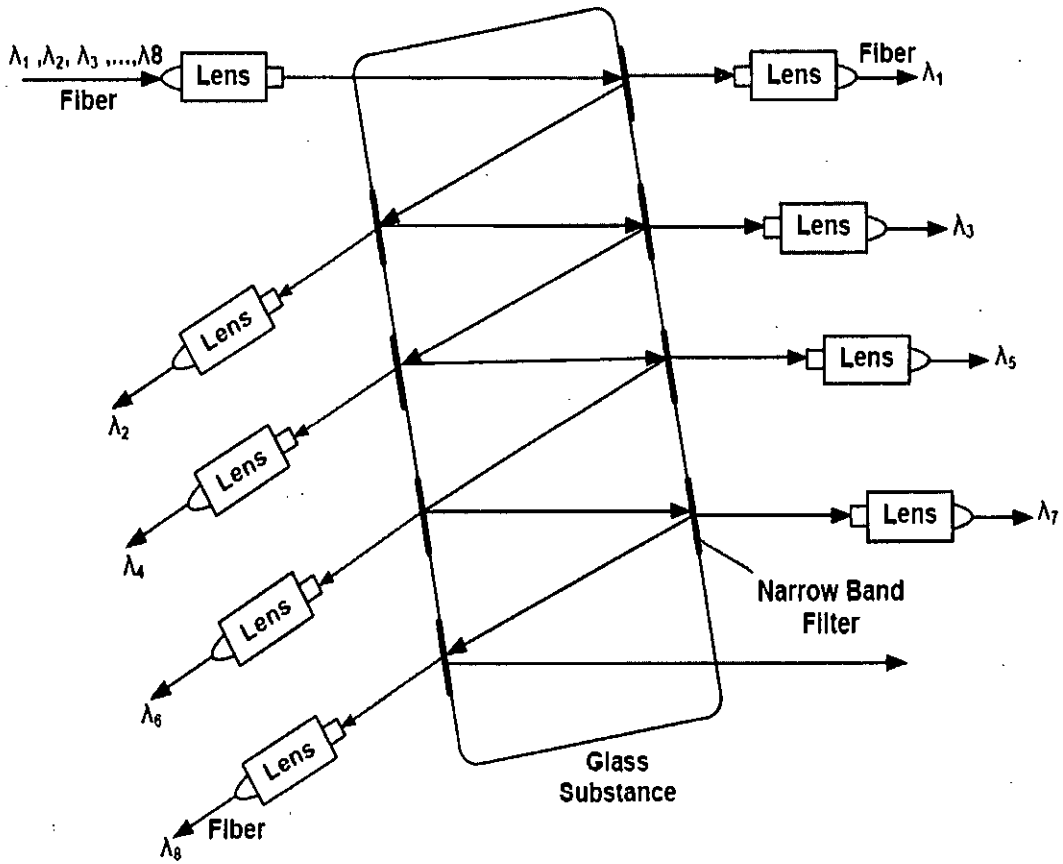
Figure 2.7: Principle of operation of TFF.

wavelength multiplexers and demultiplexers used in WDM. As well as performing basic multiplexing/demultiplexing functions, they can be combined with other components to create add/drop multiplexers.

Figure 2.8 shows the structure of an AWG. The input (a) consists of several channels, typically between 8 and 40 in commercial devices, carried on separate frequencies. Channel spacings of 100GHz or 50 GHz are common in commercial devices. The operational wavelength is commonly around 1.55μm where attenuation is lowest in optical fibres. All waveguides in the AWG tend to be single-moded to ensure predictable propagation through the device.

Light couples from the input waveguide (a) into the free propagation region (FPR) (b) and disperses to illuminate the arrayed waveguides (AWs) starting on
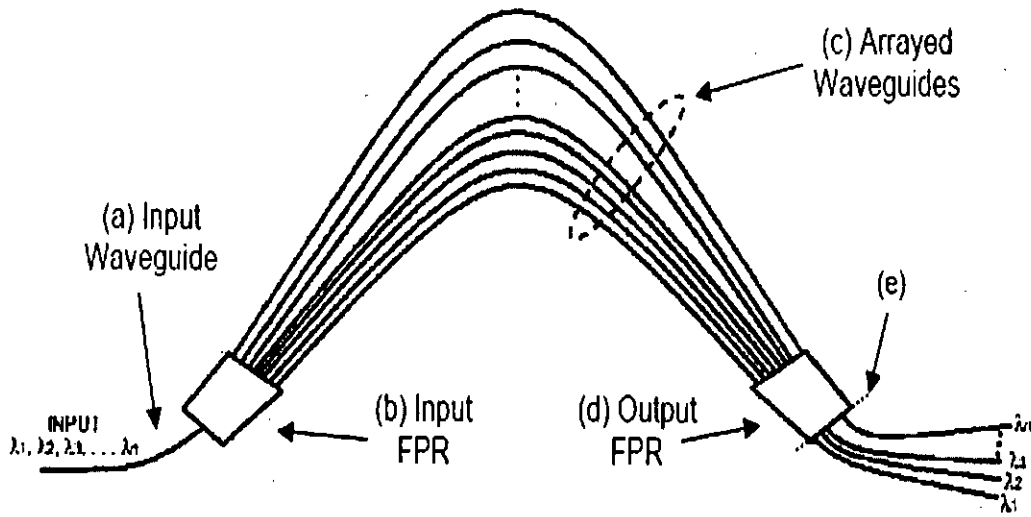
Figure 2.8: The structure of an Arrayed Waveguide Grating demultiplexer.
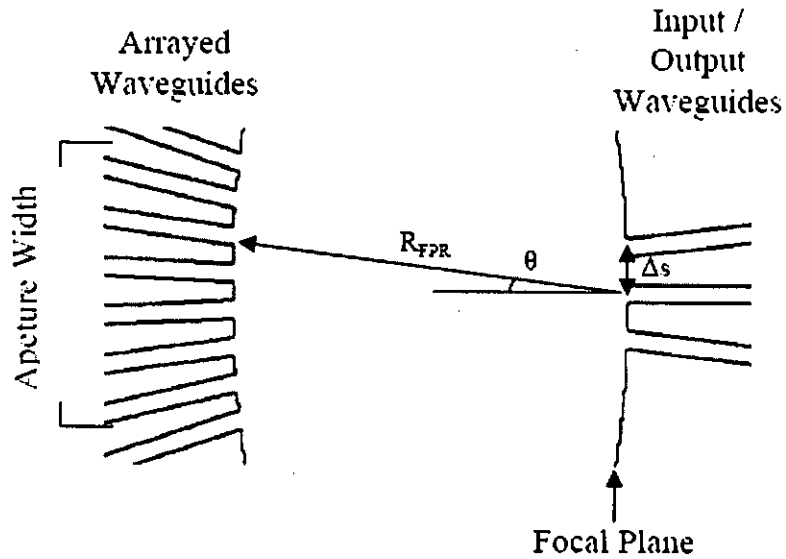
Figure 2.9: The input/output free propagation region. Δs is the displacement of focal point, R_{FPR} is the length of FPR, and θ is the dispersion angle.

a curved plane as shown in Figure 2.9, along which the light exhibits a constant phase profile. Each AW increases in length by ΔL, compared to the previous one

in the array, where $\Delta L = m\lambda_w/n_{eff}$, m is an integer number, λ_w is the central operational wavelength, and n_{eff} is the effective refractive index, β/k_0, of the single mode supported by each waveguide forming the AWG. Consequently, at the central wavelength, a constant phase profile is exhibited at the end of the AWs, an integer number of cycles out of phase, along the same plane, as shown in Figure 2.6. Therefore, at the central frequency, the light focuses at the centre of the plane (e), where an output waveguide is positioned to capture the focussed light. Different wavelengths of light will exhibit different amounts of phase change and, due to the increments in length of each waveguide, the phases will change along the AW output plane, causing the focal point to move along the focal plane (e) at the end of the FPR. An output waveguide is positioned on the output plane to pick up each input frequency (channel).

Fiber Bragg Gratings

A fiber Bragg grating is a periodic or aperiodic perturbation of the effective refractive index in the core of an optical fiber. Typically, the perturbation is approximately periodic over a certain length of e.g. a few millimeters or centimeters, and the period is of the order of hundreds of nanometers. Gratings can be formed directly within the core of silica fibers either by using holographic exposure or by using a phase mask and patterning. The two most common method of exposer are shown in Figure 2.10.
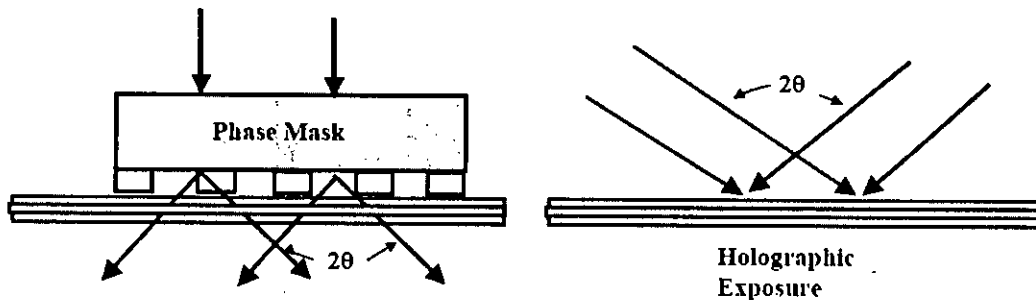
Figure 2.10: Formation of Bragg grating.

Light propagating in the core will be reflected by the interfaces between regions having different refractive indices. But the reflected light is generally out of phase

and extincts. However, for a certain wavelength, the Bragg wavelength, the light reflected by the periodically varying index of refraction will be in equal phase and added constructively. Other wavelengths are nearly not affected by the Bragg grating. Figure 2.11 shows the reflection of Bragg wavelength due to fiber Bragg grating.
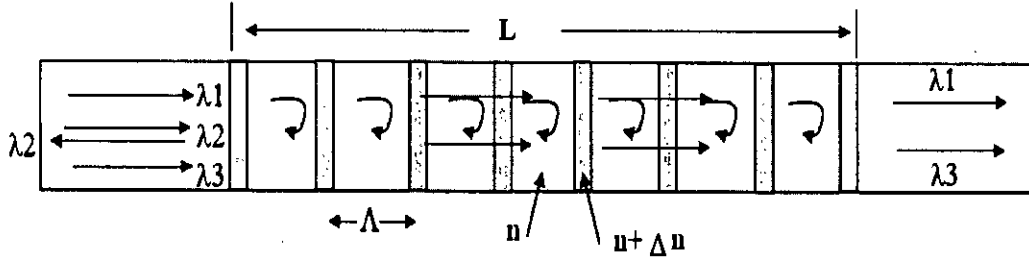
Figure 2.11: Fiber Bragg grating.

The wavelength λ_2 reflected in this case is the Bragg wavelength. The Bragg wavelength, λ_{Bragg} is defined by the relationship [17],

$$\lambda_{Bragg} = 2n_{eff}\Lambda \qquad (2.5)$$

Where n_{eff} is the average refractive index of the grating, Λ is the grating period.

The refractive index along the core is given by [17],

$$n(z) = n + \Delta n\left[1 + \cos\left(\frac{2\pi z}{\Lambda}\right)\right] \qquad (2.6)$$

where n is the unexposed core index and Δn is the photo-induced change in the index.

The peak reflectivity R_{max} for the grating of length L and coupling coefficient κ is given by [17],

$$R_{max} = \tanh^2(\kappa L) \qquad (2.7)$$

For a uniform sinusoidal modulation of the core, coupling coefficient κ is given by [17],

$$\kappa = \frac{\pi \Delta n \eta}{\lambda_{Bragg}} \tag{2.8}$$

η is the fraction of the optical power contained in the core. Under the approximation that the grating is uniform, η can be approximated by [17],

$$\eta \approx 1 - V^2 \tag{2.9}$$

where V is the V number of the fiber.

The reflection characteristics of FBG can be shown by the Figure 2.12. The
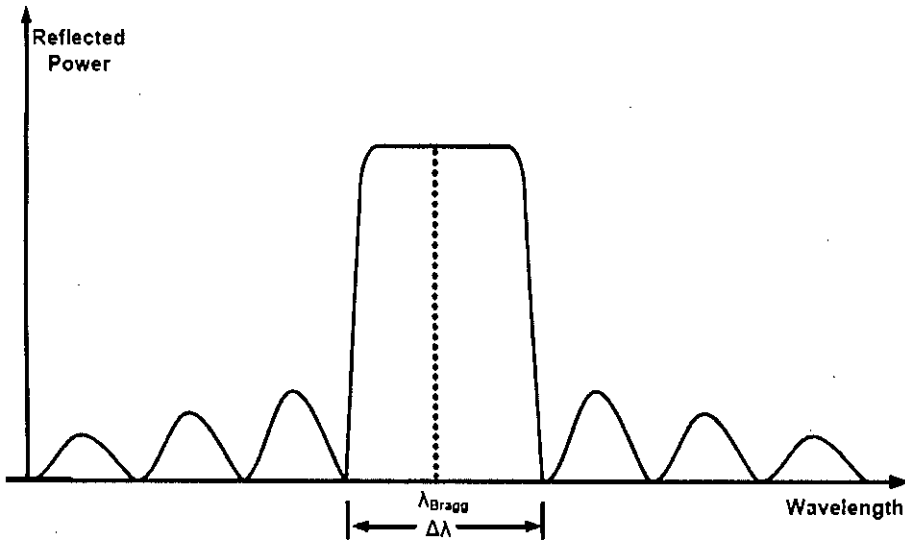
Figure 2.12: FBG's reflected power as a function of wavelength.

full bandwidth $\Delta\lambda$ over which the maximum reflectivity holds is [17],

$$\Delta\lambda = \frac{\lambda_{Bragg}^2}{\pi n_{eff} L}[(\kappa L)^2 + \pi^2]^{1/2} \tag{2.10}$$

An approximation for the full width half maximum(FWHM) bandwidth is given by [17],

$$\Delta\lambda_{FWHM} \approx \lambda_{Bragg}s\left[\left(\frac{\Delta n}{2n}\right)^2 + \left(\frac{\Lambda}{L}\right)^2\right]^{1/2} \tag{2.11}$$

where s=1 for strong grating with near 100% reflectivity.

The primary application of fiber Bragg gratings is in optical communication systems. They are specifically used as notch filters. They are also used in optical multiplexers and demultiplexers with an optical circulator, or Optical Add-Drop Multiplexer (OADM). FBG can also be tunable. In a tunable demultiplexer, the Bragg wavelength of the FBG can be tuned by strain, applied by a piezoelectric transducer.

2.1.4 Optical Fiber

A basic optical fiber communication system, shown in Figure 1.1, consists of an optical transmitter, an optical receiver and optical fiber as the communication medium. There are several other components that go into the system to make it practical, such as optical add/drop multiplexers, optical amplifiers, switches and wavelength converters.

Fiber possesses many characteristics that make it an excellent physical medium for high-speed networking. Figure 2.13 shows the two low-attenuation regions of optical fiber. A range of 200 nm is centered at approximately 1300 nm, in which attenuation is less than 0.5 dB per kilometer. The total bandwidth in this region is about 25 THz. Another region of similar size with attenuation as low as 0.2 dB per kilometer is centered at 1550 nm. Combining these two regions provide a theoretical upper bound of 50 THz of bandwidth. By using these large low-attenuation areas for data transmission, the signal loss for a set of one or more wavelengths can be made very small, thus reducing the number of amplifiers and repeaters needed. In single-channel long distance experiments, optical signals have been sent over hundreds of kilometers without amplification. Besides its enormous bandwidth and low attenuation, fiber also offers low error rates. Fiber-optic systems typically operate at bit error rates (BERs) of less than 10^{-11}.
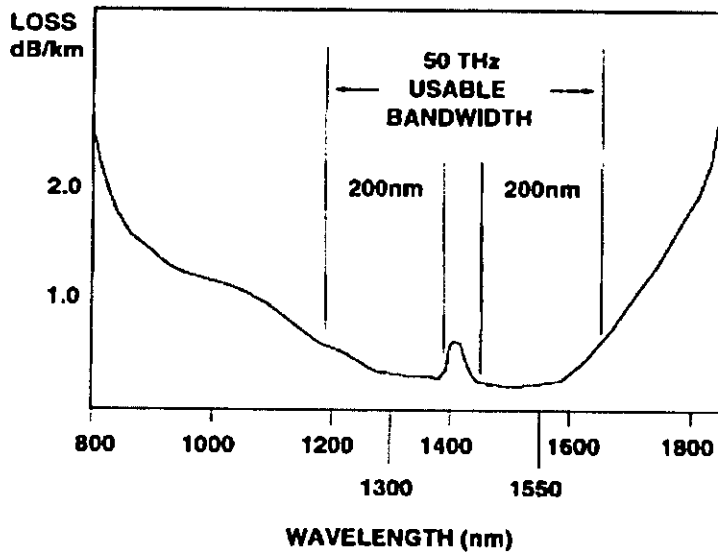
Figure 2.13: The low-attenuation regions of an optical fiber.

The small size and thickness of fiber allows more fiber to occupy the same physical space as copper, a property that is desirable when installing local networks in buildings. Fiber is flexible, difficult to break, reliable in corrosive environments, and deployable at short notice (which makes it particularly favorable for military communications systems). Also, fiber transmission is immune to electromagnetic interference and does not cause interference. Last, fiber is made from one of the cheapest and most readily available substances on earth, sand. This makes fiber environmentally sound; and unlike copper, its use will not deplete natural resources.

There are two general types of optical fiber: singlemode and multimode fiber. Singlemode fiber has a very smaller core diameter of 8 to 10 μm, and it allows only one mode of light to transport through the core without modal dispersion or pulse spreading. Thus singlemode fiber provides an unlimited bandwidth carrying capacity in data transmission, especially in high speed and long-haul distribution. Multimode fiber has a much larger core size of 50 to 80 μm while it supports hundreds of paths of light from different angles. Based on this design, multimode fiber is more suitable for lower speed and short distance transmission.

The dispersion and nonlinear effect of optical fiber has a significant impact on the performance of WDM system. Considering these effects the pulse propagation through the optical fiber is given by the nonlinear Schrodinger equation (NLSE). The modified NLSE is given by [22],

$$i\frac{\partial A}{\partial z} = -\frac{i}{2}\alpha A + \frac{1}{2}\beta_2\frac{\partial^2 A}{\partial T^2} + \frac{i}{6}\beta_3\frac{\partial^3 A}{\partial T^3} - \gamma|A|^2 A \qquad (2.12)$$

where A is the slowly varying amplitude of pulse envelope, β_2 and β_3 are the second and third order dispersion respectively, α is the fiber attenuation, γ is the fiber nonlinearities, and T is the time reference moving with the pulse.

2.1.5 Optical Amplifiers

Optical amplifiers(OAs) boost optical signals in the optical domain to minimize the effects of power loss and attenuation that result from sending light pulses over optical fiber. Optical amplifier (OA) technology is the key to enabling the high speed, high-volume transmission of WDM to take place. OA involves two types: the semiconductor laser type amplifier (SOA) and the fiber type amplifier such as erbium-doped fiber amplifier (EDFA). Furthermore, there are some physical nonlinear effects inside the optical fiber which can be stimulated and utilized in transferring photonic energy from a source laser to an objective weak signal such as Brillouin scattering and Raman scattering amplifiers.

Before the advent of optical amplifiers, each signal had to be regenerated electronically. While regenerating an optical signal electronically, the signal must first be converted to an electrical signal, amplified, and then converted back to an optical signal before being retransmitted. Electronic regeneration requires a separate regenerator for each wavelength on each fiber. However, a single optical amplifier can amplify all of the wavelengths on one fiber.

The most common type of optical amplifier is the erbium doped fiber amplifier (EDFA). Conventional EDFAs operate in the 1530 to 1560 nm range. The element erbium boosts the power of wavelengths and eliminates the need for regeneration. Optical pump lasers are used to transfer high levels of energy to the
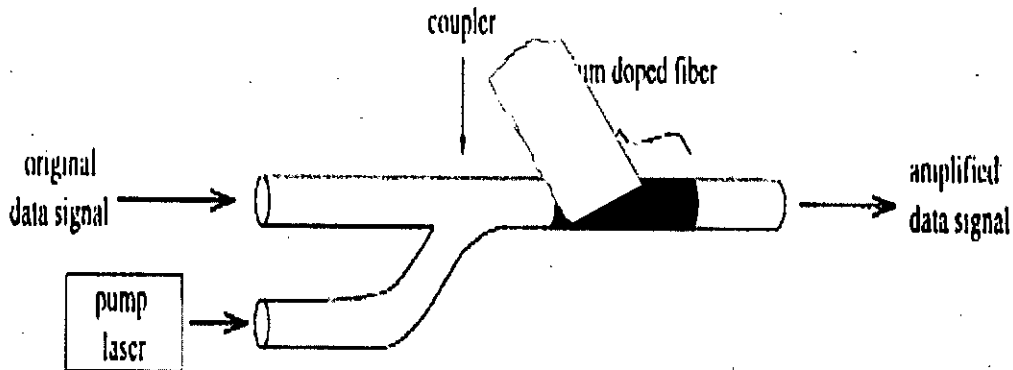
Figure 2.14: A simple EDFA structure.

special fiber, energizing the Erbium ions, which boosts the optical signals that are passing through the doped fiber as shown in Figure 2.14. Instead of multiple electronic regenerators, which require that the optical signals be converted to electrical signals then back again to optical ones, the EDFA directly amplifies the optical signals. Hence the composite optical signals can travel up to 600 kms without regeneration and up to 120 kms between amplifiers, in a commercially available terrestrial WDM system. The significance of OA is that, it improves the operating transparency during the signal amplification process. In addition, it has a big impact on reducing the system complexity of the entire fiber communication system. The limitation of OA is that reshaping, retiming and other signal processing are not possible by OA, only amplification is possible.

2.1.6 Circulators

An optical circulator(OC) is a non reciprocal device allowing for the routing of light from one fiber to another based upon the direction of the light propagation. Nonreciprocal optical devices, such as optical isolators and optical circulators, are essential components of optical communication systems. Optical isolators pass light, propagating in a forward direction while inhibiting the propagation of light in a backward direction. Optical circulators enable the routing of light from one optical fiber or waveguide to another based upon the direction of light propagation.
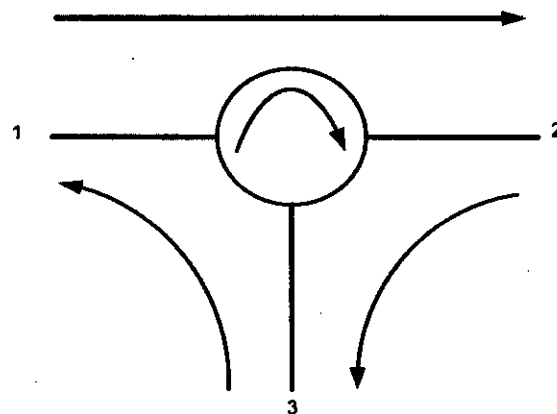
Figure 2.15: A 3 port optical circulator.

A circulator has at least three optical ports. These ports can be accessed in such order that, when a light beam is caused to enter into an optical port, this light-beam after passing through the circulator exits from a next optical port. The light enters the circulator through a first port and exits through a second port. Another light that enters the second port exits through a third port and so on. A three port optical circulator is shown in Figure 2.15. Since the optical circulator is an inherently non-reciprocal device, the light never goes to other ports. When one port of a three-port circulator is terminated in a matched load, it can be used as an isolator, since a signal can travel in only one direction between the remaining ports. Optical circulators have wide applications. They are used to convert an existing unidirectional fiber optic communication link to a full duplex communication link by installing an optical circulator at each end of the link. Optical circulators are also used ill fiber amplification systems and wavelength division multiplex (WDM) networks.

2.1.7 Wavelength Converters

A wavelength converter is a device capable of switching data from an input port on one wavelength λ_1 to an output port on another wavelength λ_2. Wavelength

converters are very useful in reducing the blocking probability of the network. If wavelength converters are included in the cross-connects in WDM networks, connections can be established between the source and the destination even when the same wavelength is not available on all the links in the path. Wavelength converters help to eliminate the wavelength-continuity constraint. The following are some of the characteristics that an ideal wavelength converter should possess.

1. Transparency to bit rates and signal formats.

2. Fast setup time of output wavelength.

3. Conversion to both shorter and longer wavelengths.

4. Moderate input power levels.

5. Insensitivity to input signal.

6. Simple implementation.
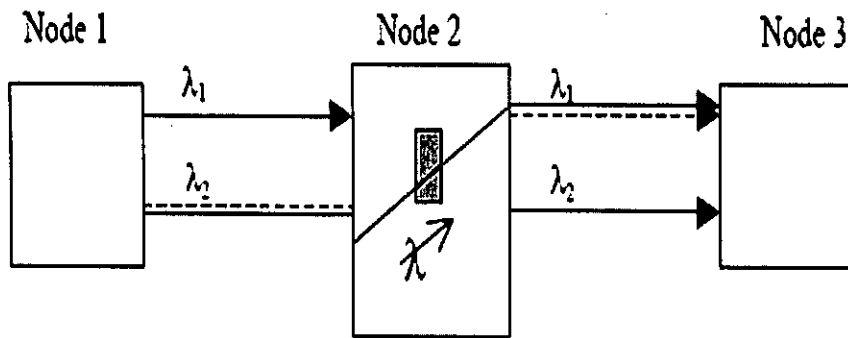
Figure 2.16: The use of wavelength converter.

In Figure 2.16, a lightpath is established between Node 1 and Node 2 on wavelength λ_1 and another lightpath is established between Node 2 and Node 3 on wavelength λ_2. Now if a request arrives at Node 1 destined to Node 3, the request cannot be accepted because of the wavelength-continuity constraint. But if we have a wavelength converter placed at Node 2 that can convert wavelength λ_1 to λ_2, then the request can be successfully honored. Clearly wavelength converters

can help in improving the performance when free wavelengths are available on links, and a common wavelength is not available. A wavelength converter used to perform this function is sometimes called a transponder.

Wavelength converters can be divided into two types based on the amount of conversion possible. A full-wavelength converter is one that can convert an input wavelength into any of the outgoing wavelengths. A limited-wavelength converter is one that can convert an input wavelength only to a subset of the outgoing wavelengths. A network that has full-wavelength converters at all the nodes will perform well with respect to minimizing the blocking probability. However, this is difficult to implement in practice because of the cost factor and also due to technological limitations.

Wavelength conversion implementation can be broadly classified into two types: opto-electronic wavelength conversion and all-optical wavelength conversion. In opto-electronic method, the optical signal to be converted is first converted into the electronic domain using a photo detector. The electronic bit stream is stored in a buffer. The electronic signal is then used to drive the input of a tunable laser tuned to the desired wavelength of the output. This method is not suitable for higher bit rates. Data rates of up to 10 Gbps have been demonstrated with this method. Consumption of more power and complex procedure are some of the other drawbacks of this method when compared to other methods. Moreover, the process of opto-electronic (O-E) conversion adversely affects transparency. In all-optical method, the optical signal is in the optical domain through out the conversion process.

2.1.8 Optical Switches

Optical switches are used in optical network for variety of applications. Different applications require different switching times and switching ports. One application of optical switches is the provisioning of lightpaths. In this application the switches are used inside the optical cross-connects (OXC) to reconfigure them to support new lightpaths. For this application, switches with millisecond switching times are acceptable.

Another application is that of protection switching. Here, the switches are used to switch the traffic stream from a primary fiber onto another fiber in case the primary fiber fails. Switching time required for this purpose is of the order of few milliseconds.

Switches are also important in high speed optical packet-switched networks. In these networks, switches are used to switch signals on a packet basis. Switching time for this application must be smaller than a packet duration.

Another use for switches is as an external modulator to run on and off the data in front of a laser source. In this case, the switching time must be a small fraction of the bit duration.

Important parameters used to characterize the suitability of a switch for optical networking are as follows:

1. The extinction ratio is the ratio of the output power in the on state to the output power in the off state.It should be as large as possible.

2. The insertion loss is the fraction of power that is lost because of the presence of the switch.It should be as small as possible.

3. Crosstalk is the power leaking to the desired output from other inputs than the desired input.It should be minimum.

2.1.9 Receivers

An optical receiver is the converter of optical power, μW to electrical current, mA. Figure 2.17 shows an optical receiver with the photodetector as its key element. The goal of the receiver is to receive the optical signal and convert into the binary digit. The expression of bit error rate in absence of different receiver noises is derived in section 3.6. Here we describe different types of noises that is present in the optical receiver.
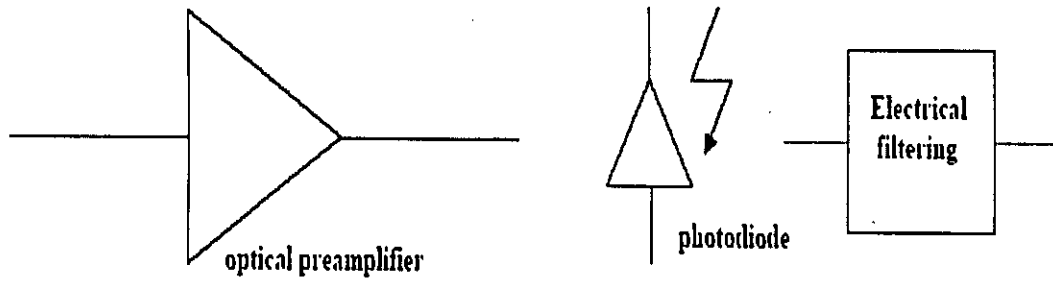
Figure 2.17: A simple optical receiver.

Shot Noise

The shot noise is due to the photodiode and is related to quantum characteristics of photocurrent. Its expression is given by [21],

$$\sigma^2_{shot} = 2\eta e B_e(GI_s + MI_N) \qquad (2.13)$$

Where,

G=gain of the amplifier,

η=quantum efficiency,

B_e=electrical bandwidth of the receiver,

I_s=photocurrent due to optical signal,

I_N= ASE noise current corresponding to the noise power P_{ASE}, and

M=number of ASE modes.

Thermal Noise

The thermal noise is associated to the electronic circuit of the receiver and is defined by [21],

$$\sigma^2_{th} = \frac{4kTB_e}{R_L} \qquad (2.14)$$

where,

k = Boltzman constant,

T = Room temperature in degree Kelvin,

B_e = Receiver electrical bandwidth in Hz, and

R_L = Resistance of the load bus in ohm

Amplified Spontaneous Emission

The amplified spontaneous emission (ASE) noise is generated within the optical amplifiers. This is a wide band noise so it will be considered to have the same spectral density above the whole optical bandwidth B_o of the amplifier. The expression of its power is given by [21],

$$P_{ASE} = h\eta G n_{eq} B_o \qquad (2.15)$$

where,

n_{eq}=equivalent input noise factor,

h=Planck's Constant, and

B_o=optical bandwidth of the receiver.

The ASE noise causes beat noise with the signal and with the ASE itself. The signal-ASE beat noise is given by [21],

$$\sigma^2_{S-ASE} = 4\eta^2 G P_s P_{ASE} \frac{B_e}{B_o} \left(\frac{e}{h\upsilon}\right)^2 \qquad (2.16)$$

where,

P_s = input signal power,

υ = signal frequency, and

other parameters are defined above.

The ASE-ASE beat noise is due the beat of the spontaneous emission noise with itself. Its expression is given by [21],

$$\sigma^2_{ASE-ASE} = M\eta^2 P^2_{ASE} \frac{B_e}{B_o^2}(2B_o - B_e)\left(\frac{e}{h\upsilon}\right)^2 \qquad (2.17)$$

Total Receiver Noise

Total receiver noise can be expressed as found from equation [2.13 - 2.17] by [21],

$$\sigma^2 = \sigma^2_{th} + \sigma^2_{shot} + \sigma^2_{S-ASE} + \sigma^2_{ASE-ASE} \qquad (2.18)$$

2.2   WDM Network Elements

A WDM network consists of the following elements:

1. Optical Line Terminals (OLTs)

2. Optical Add/Drop Multiplexers (OADMs)

3. Optical Cross-Connects (OXCs)

2.2.1   Optical Line Terminals
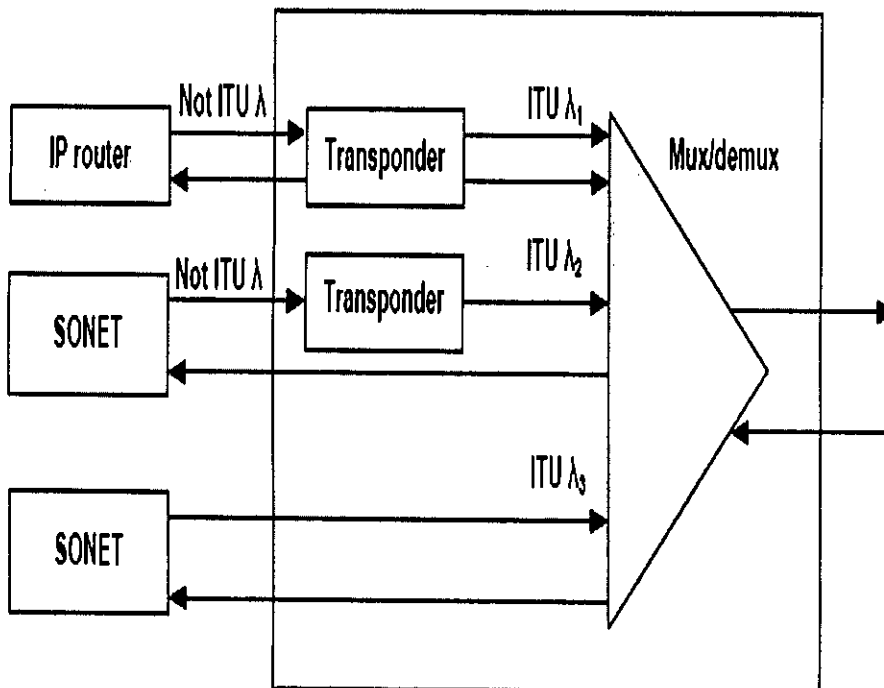
Figure 2.18: Block diagram of an optical line terminal.

OLTs are normally used at either end of a link to adapt the signals and to multiplex/demultiplex wavelength channels. Three functional devices may be included in an OLT, as shown in Figure 2.18.

1. A transponder adapts the incoming signal into a signal suitable for the network regarding signal level and wavelength.

2. Wavelength mux/demux is used to combine and separate wavelengths.

3. OLTs also add and terminate an optical supervisory channel (OSC), carried on a separate wavelength. It is used to monitor the performance of the devices along a link.

2.2.2 Optical Add/Drop Multiplexers
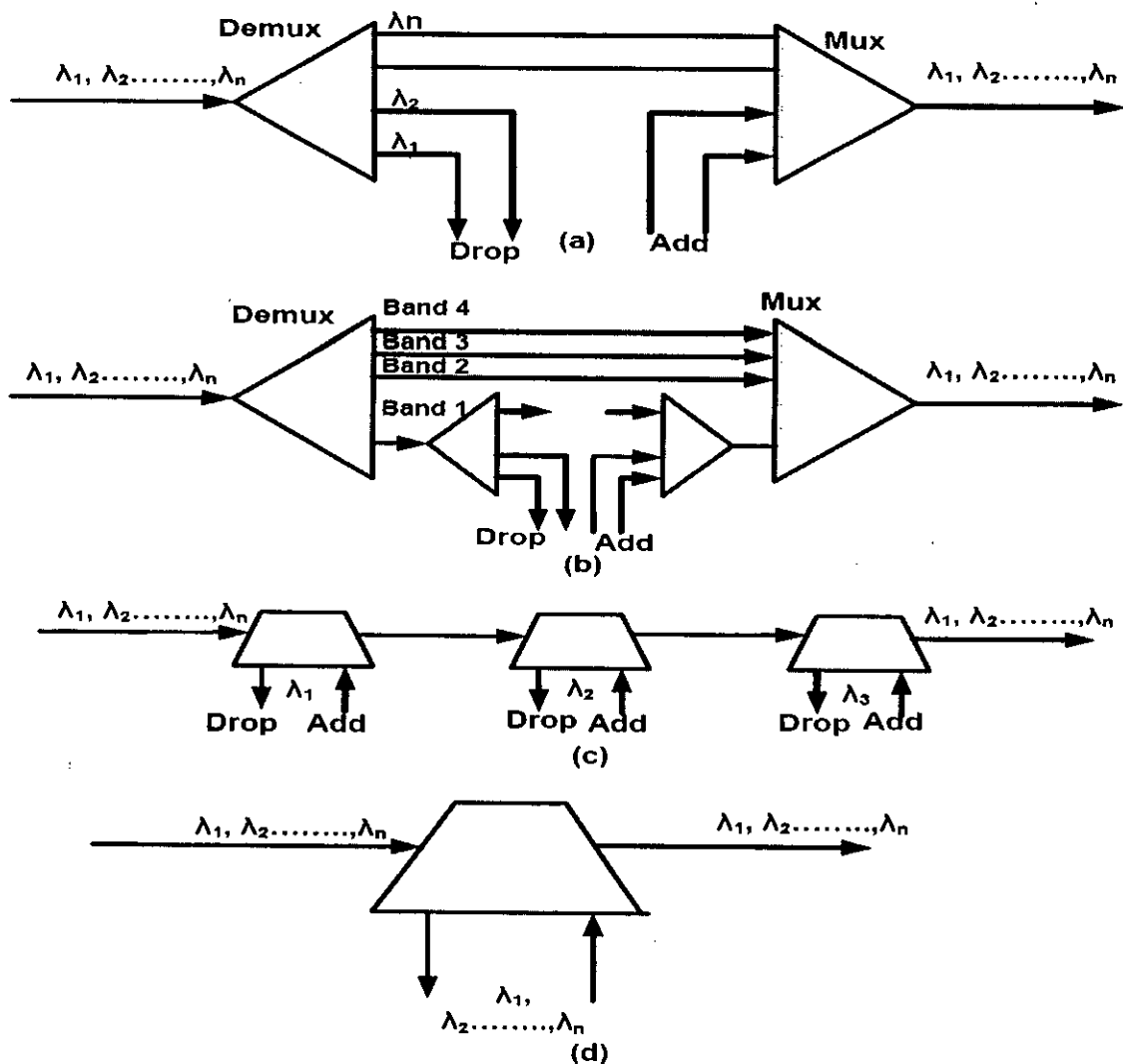
Figure 2.19: Different OADM architectures. (a) parallel; (b) modular version of (a);(c) serial; and (d) band drop.

An optical add/drop multiplexer (OADM) is a device used in WDM systems for multiplexing and routing different channels of light into or out of a single mode fiber (SMF). This is a type of optical node, which is generally used for the construction of a ring-based optical telecommunications network. "Add" and "drop" here refer to the capability of the device to add one or more new wavelength channels to an existing multi-wavelength WDM signal, and/or to drop (remove) one or more channels, routing those signals to another network path. Figure 2.19 shows different OADM architectures. In (a), all the wavelengths are separated and multiplexed back together, in (c), wavelengths are dropped and added one at a time and in (d), a band of wavelengths are dropped and added together.

2.2.3 Optical Cross-Connects

The nodes of a network basically consist of OXCs, that guide light from one link to another. OXCs are the key elements enabling reconfigurable optical networks. As compared with an OADM, the OXC is advantageous for complex mesh networks or a large number of wavelengths. Figure 2.20 shows different scenarios for OXC deployment. The scenerios differ in terms of whether the actual switching is done electrically or optically, in the use of optical to electrical (O/E) and optical to electrical to optical (O/E/O) converters and how the OXC is interconnected with the surrounding equipment.

OXCs need not be all-optical, internally they can use either an electrical or an optical switch fabric. It consists of a switch core that performs the actual cross-connecting and a port complex being used as an interface between the OLTs and the switch core, providing O/E-conversion, O/E/O-conversion, or no conversion. Further, it may be opaque or transparent. Interconnection between the OLTs and the OXCs, as well as inside the OXCs, are often done through short-reach interfaces at a shorter wavelength, typically at 1310 nm.

An optical switch core is bit rate transparent, offering a more scalable capacity (TDM). The cost for an electrical port increases with the bit rate, while an optical port is bit rate independent, thus becoming more cost efficient at high bit rates. OXCs can also do the add/drop operation.
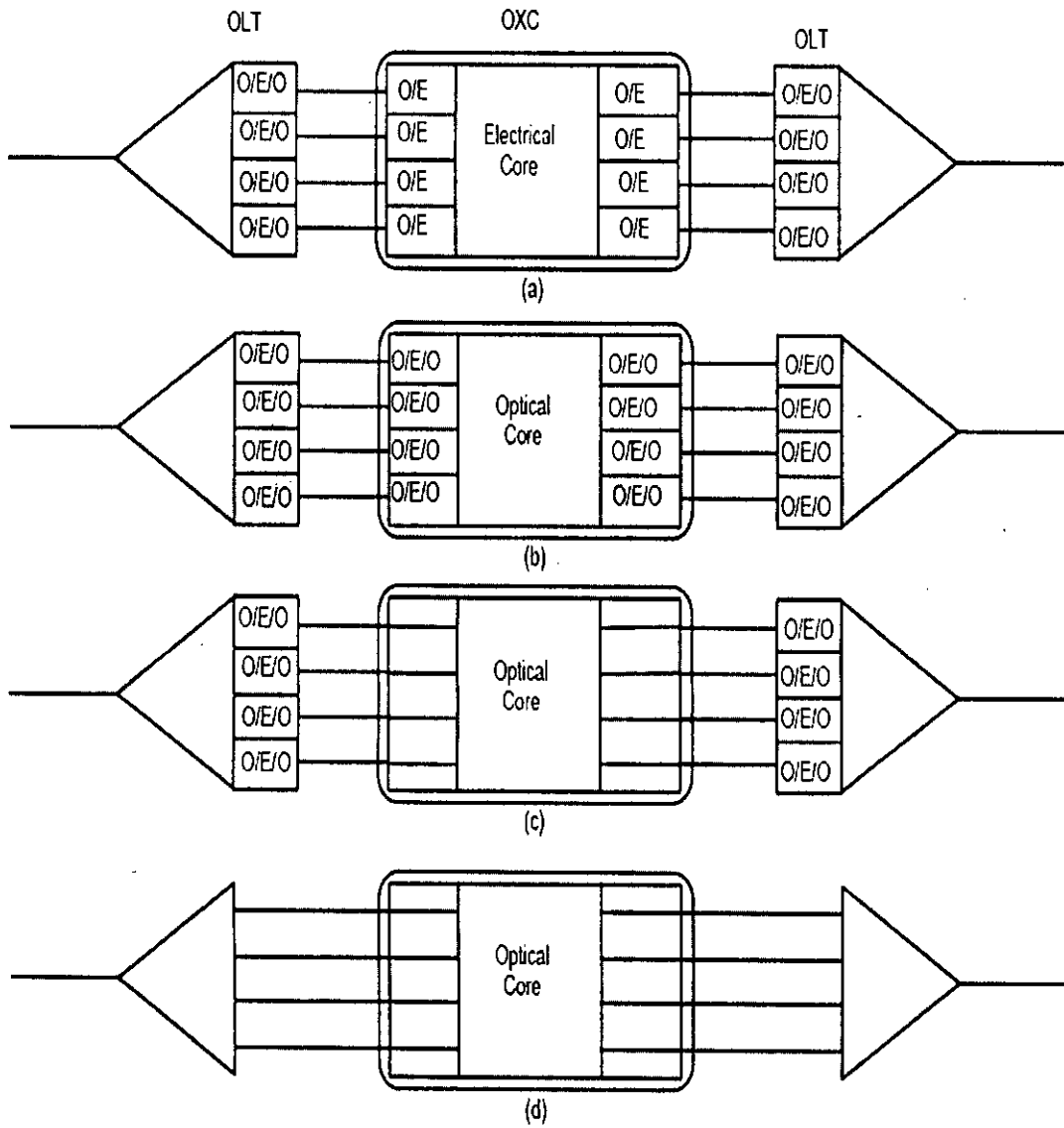
Figure 2.20: Different OXC deployment. (a) electrical switch core;(b) optical switch core surrounded by optical to electrical to optical (O/E/O) converters;(c) optical switch core directly connected to transponder;(d) optical switch core directly connected to mux/demux.

2.3   Modeling of the system

Figure 2.21 shows the system model of a WDM network using unidirectional OXCs. Each input multiplexer combines M wavelengths coming from the M transmitters, and is connected through the fiber to the input port of the OXC, the detail view of which is given in Figure 2.22. The OXC uses N number of $(M \times 1)$ multiplexers
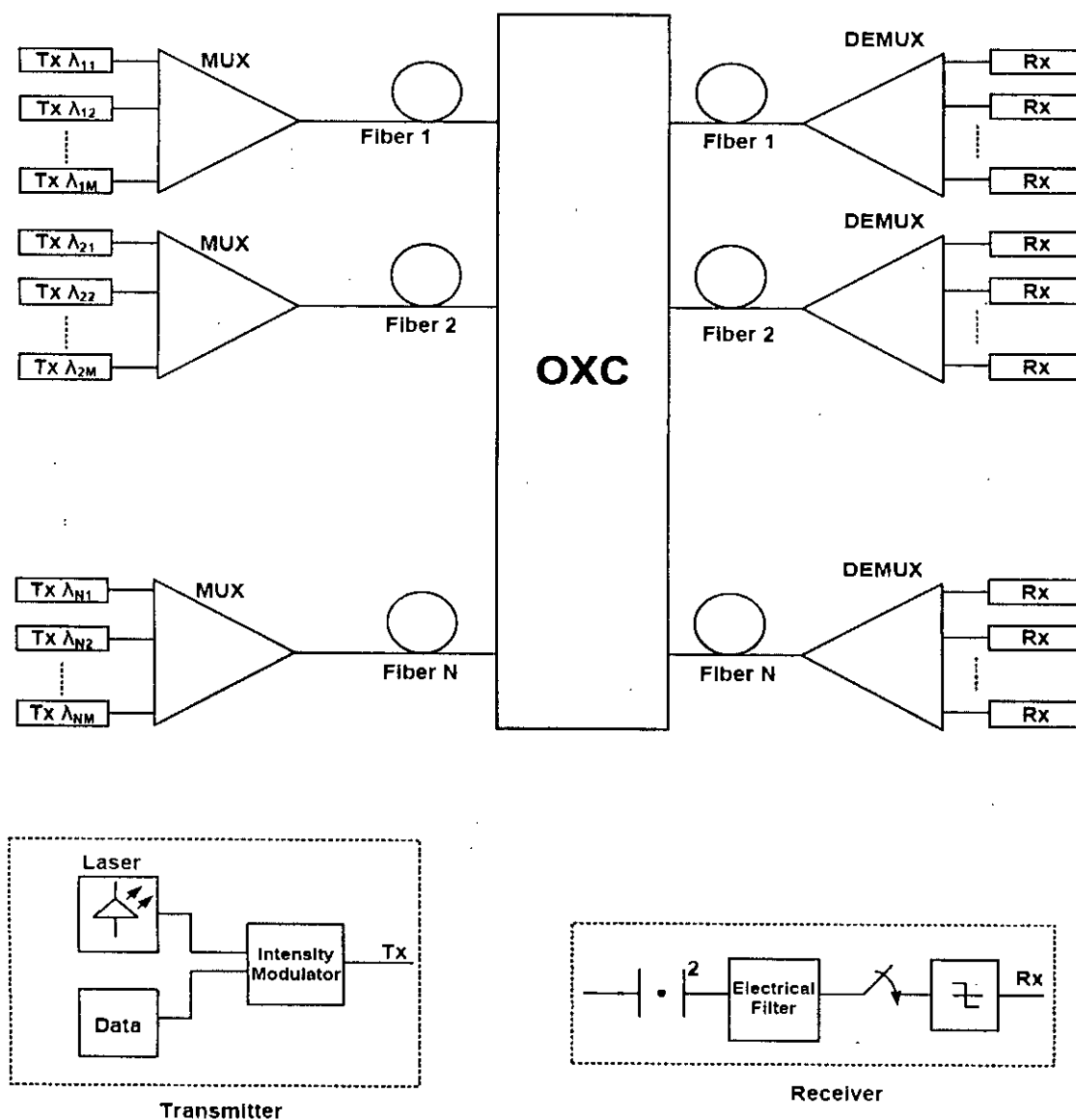
Figure 2.21: Modeling of a WDM system using unidirectional OXC.

and $(1 \times M)$ demultiplexers and M number of $(N \times N)$ optical switches. The demultiplexer of OXC separates M wavelengths. The optical switch takes N number of same wavelength signal coming from all the N input fibers and connect each wavelength to any of the N output fibers according to the destination address. The multiplexer of OXC again combines M number of wavelengths and send them
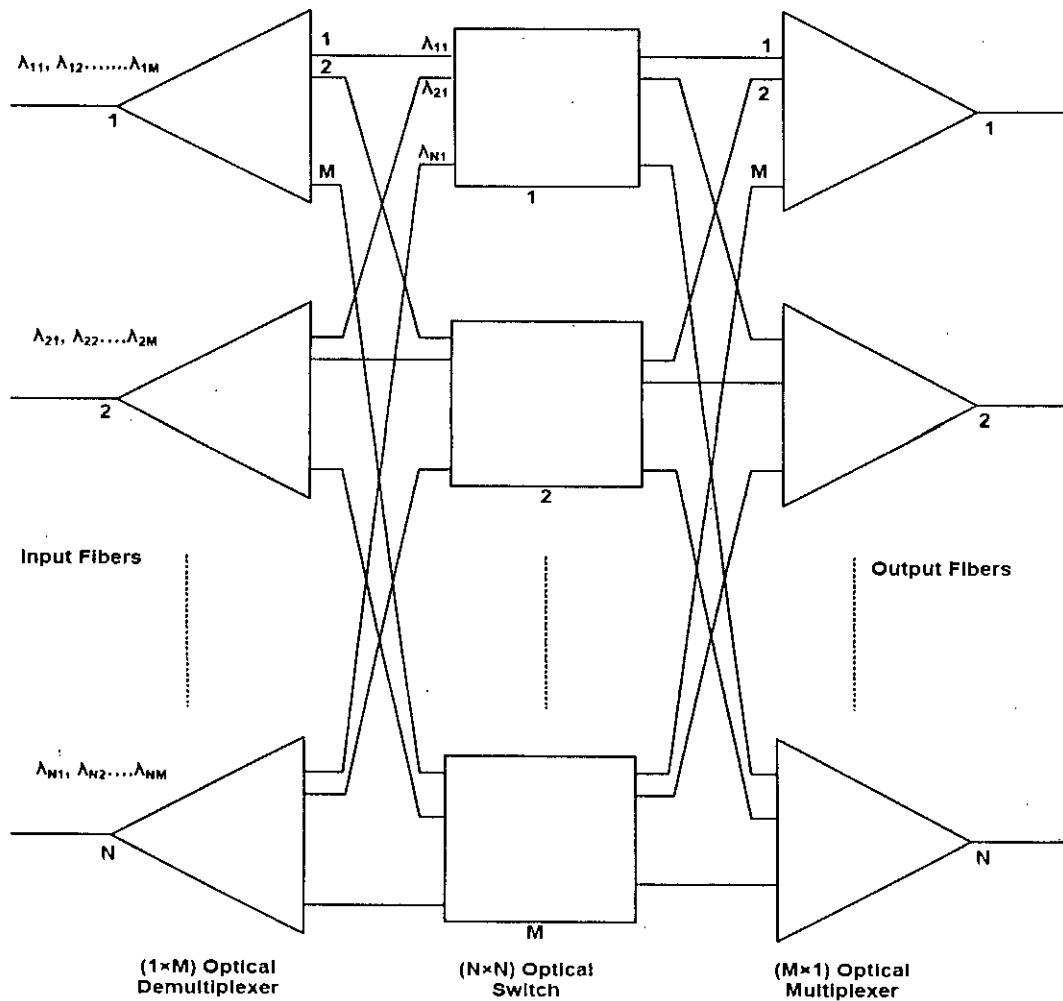
Figure 2.22: Conventional OXC using mulitplexer, demultiplexer and optical switch. This OXC has N input and output fibers with M wavelengths per fiber.

to a single fiber. The output demultiplexer separates the M wavelengths and send them to the individual user terminal.

Figure 2.23 shows the model of a WDM system for bidirectional communication using BOXC. Transmission and receiption is done at the same node. Multiplexing and demultiplexing is also done by the same device as shown in the figure. Different
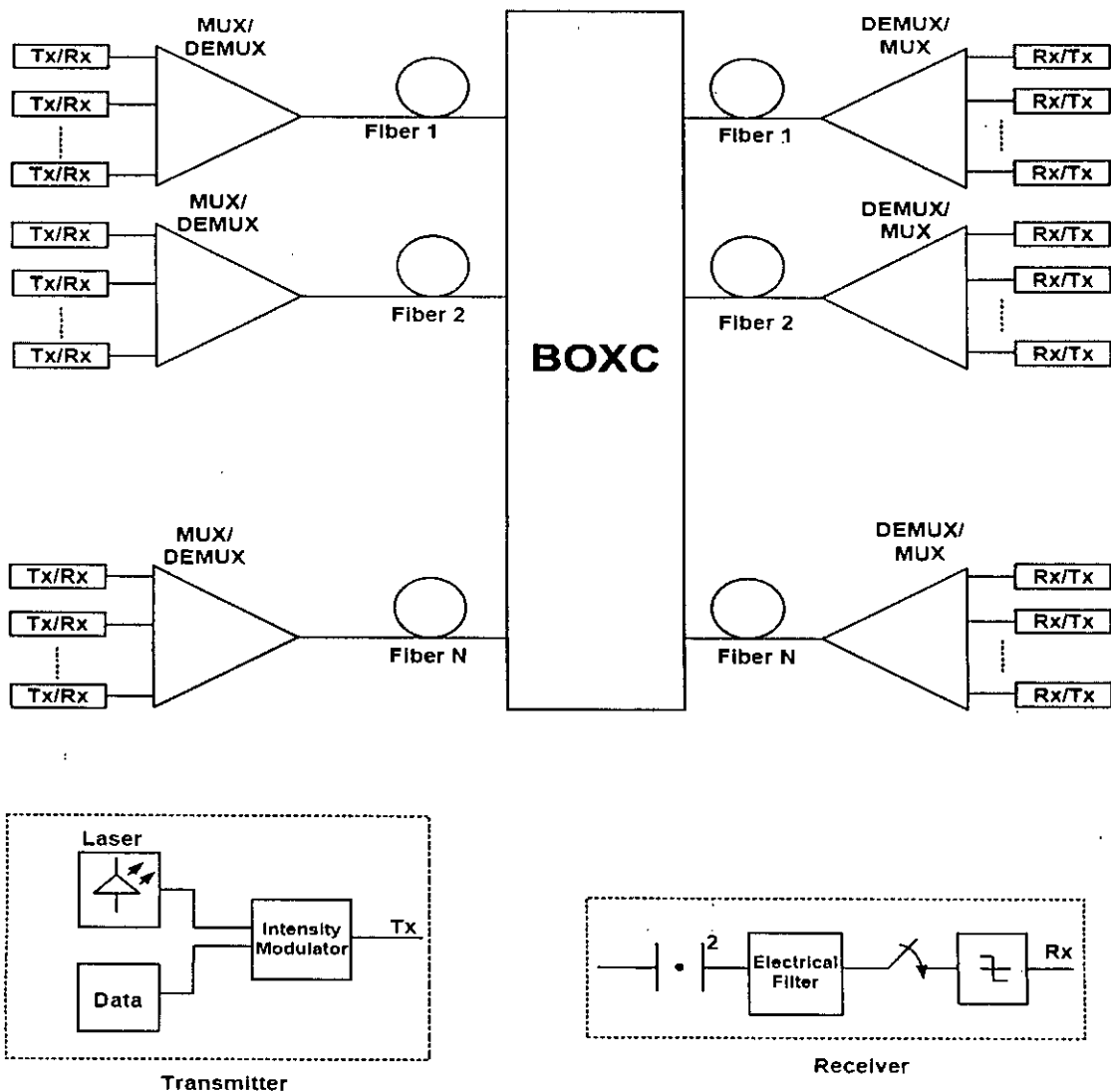
Figure 2.23: Modeling of a WDM system using bidirectional OXC. BOXCs allow switching any wavelength from any input fiber to any output fiber and vice versa.

configurations of BOXCs are given in [11]- [16]. BOXCs can be realized [14] by using conventional OXCs and optical couplers as shown in Figure 2.24. An $N \times N$ BOXC can be realized by cascading this 2×2 BOXC.
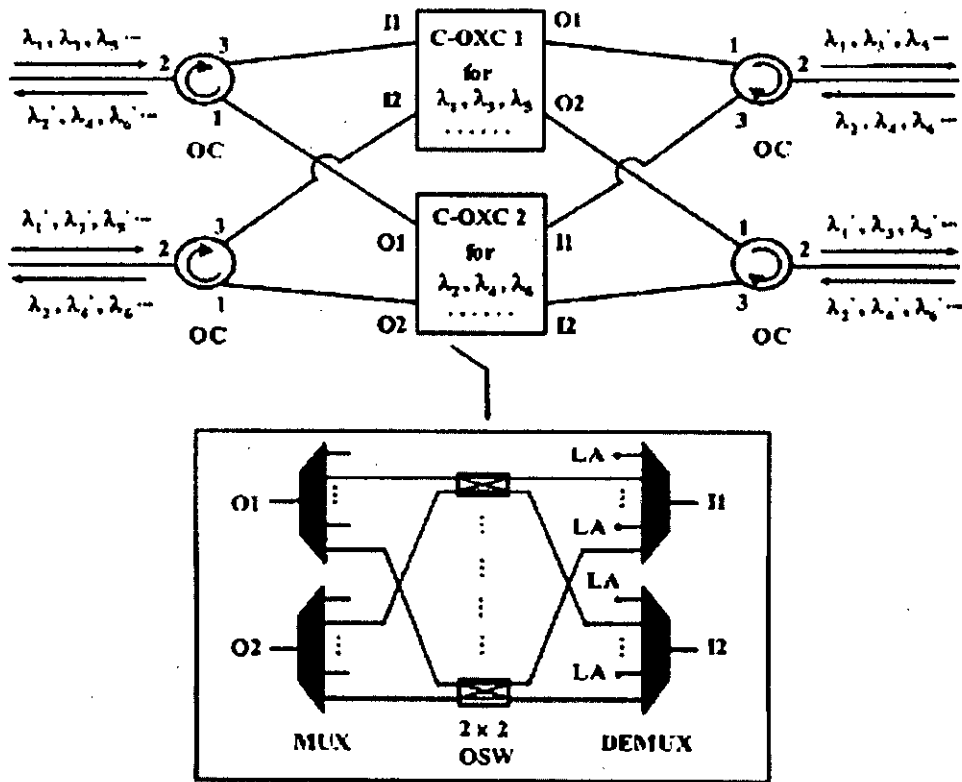
Figure 2.24: Schematic diagram of a 2 × 2 BOXC using conventional OXCs (C-OXCs) and couplers. Inset: Structure of C-OXC (LA:Light Absorber, OSW:Optical Switch, and OC:Optical Circulator.

2.4 Summary

Two models of WDM system for unidirectional and bidirectional optical fiber communication have been given in this chapter. Before presenting these models, for better understanding, different WDM components and network elelments are described briefly in this chapter.

Chapter 3

Theoretical Analysis of Crosstalk

This chapter starts with the classification of different types of crosstalk that is present in optical network. The theory, analytical expression and the impact on the BER performance of these different types of crosstalk in WDM systems are described elaborately.

3.1 Introduction

Crosstalk is the general term given to the effect of other channel on the desired signal. Almost every component in a WDM system introduces crosstalk of some form or another. The components include filters, wavelength multiplexers/demultiplexers, switches, semiconductor optical amplifiers, and the fiber itself (by way of nonlinearities).

3.2 Classification of Optical Crosstalk in WDM Systems

Several types of crosstalk can be distinguished in optical networks. Optical crosstalk can be broadly classified into non-linear and linear types. Figure 3.1 shows schematically different types of crosstalk that may arise in a WDM network. We will consider only the linear type of crosstalk in our analysis. Linear crosstalk is caused entirely by non-ideal performance of an optical node. Different types of linear
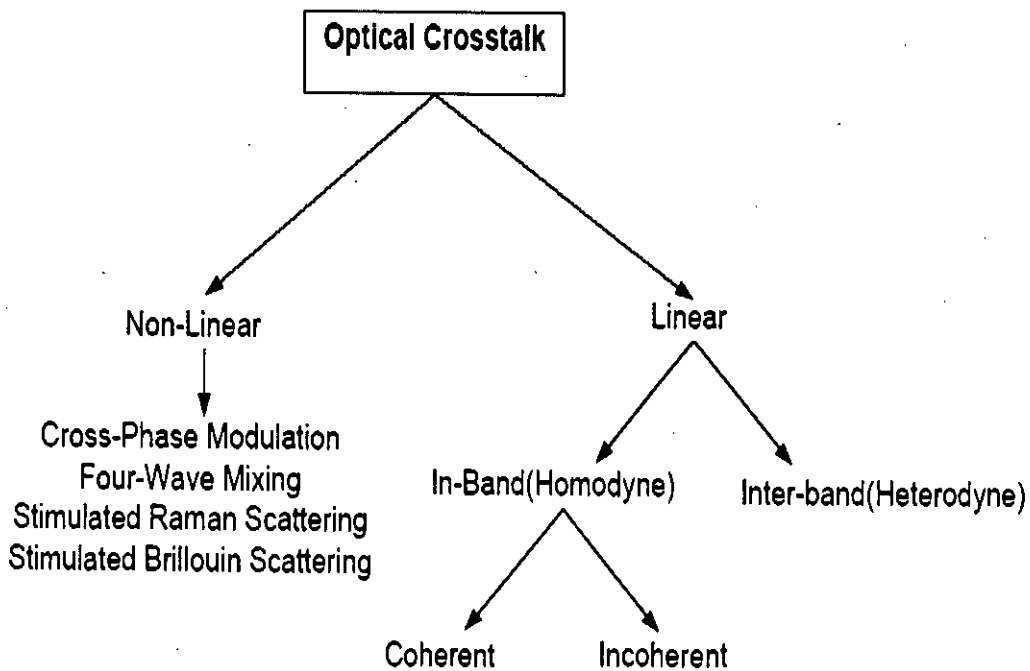
Figure 3.1: Overview of different types of optical crosstalk in WDM networks.

crosstalk are described below.

3.2.1 In-Band Crosstalk

When the crosstalk signal is at the same wavelength as that of the desired signal or sufficiently close to it that the difference in wavelength is within the receiver's electrical bandwidth, it is called in-band crosstalk. This form of crosstalk is also called as intrachannel crosstalk or homodyne crosstalk. In-band crosstalk is a major problem in optical networks. One source of this arises from cascading a wavelength demultiplexer (demux) with a wavelength multiplexer (mux) as shown in Figure 3.2. The demux ideally separates the incoming wavelengths to different output fibers. In reality, however a portion of the signal at one wavelength, say, λ_i, leaks into the adjacent channel λ_{i+1} because of non ideal suppression within the demux. When the wavelengths are combined again into a single fiber by the mux, a small portion of the λ_i, that leaked into the λ_{i+1} channel, will also leak
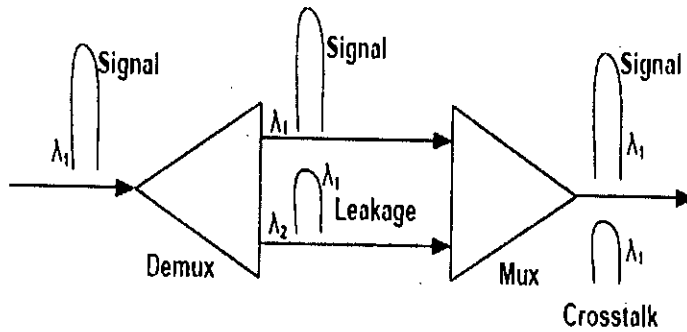
Figure 3.2: A cascaded wavelength demultiplexer and multiplexer as a source of in-band crosstalk

back into the common fiber at the output. Although both signals contain the same data, they are not in phase with each other, due to different delays encountered by them. This causes in-band crosstalk.
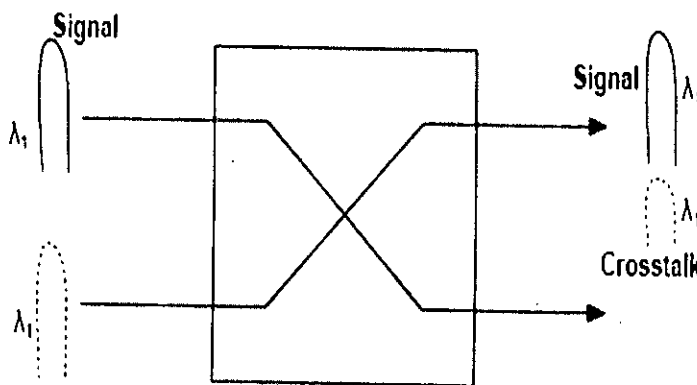
Figure 3.3: An optical switch as a source of in-band crosstalk.

Another source of this type of crosstalk arises from optical switches, as shown in Figure 3.3, due to the non ideal isolation of one switch port from the other. In this case, the signal contain different data. The crosstalk penalty is highest when the crosstalk signal is exactly out of phase with the desired signal.

Homodyne crosstalk can be divided into coherent crosstalk and incoherent crosstalk. When the phase of the crosstalk signal is correlated with that of the main signal, it is called coherent crosstalk. When the phase of the crosstalk signal is not correlated with that of the main signal, it is called incoherent crosstalk. Crosstalk signals generated from the same source are coherent crosstalk and crosstalk signals generated from different sources are incoherent crosstalk. Coherent crosstalk is believed not to causes noise but causes fluctuations of signal power [7].

3.2.2 Inter-Band Crosstalk
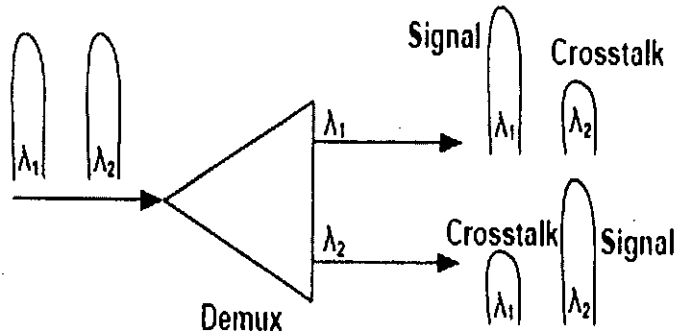
Figure 3.4: An optical demultiplexer as a source of inter-band crosstalk.

When the crosstalk signal is at a wavelength sufficiently different from the desired signal's wavelength that the difference is larger than the electrical bandwidth of the receiver, it is called inter-band crosstalk. This form of crosstalk is also called as inter channel crosstalk or heterodyne crosstalk. Inter channel crosstalk can arise from a variety of sources. A simple example is an optical filter or demultiplexer that selects one channel and imperfectly rejects the others as shown in Figure 3.4. Another example is an optical switch, switching different wavelengths shown in Figure 3.5, where the crosstalk arises because of imperfect isolation between the switch ports.
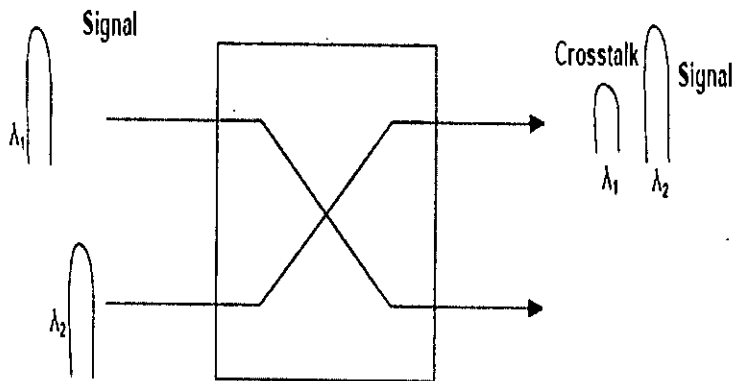
Figure 3.5: An optical switch with inputs at different wavelengths as a source of inter-band crosstalk.

3.2.3 Bidirectional System

In a bidirectional transmission system, data is transmitted in both direction over a single fiber, as shown in Figure 3.6. Although the laws of physics do not prevent the same wavelength from being used in both directions of transmissions, this is not a good practice because of reflections. A back-reflection from a point close to the transmission at one end, say, A, will send a lot of power back into A's receiver, creating a large amount of crosstalk.
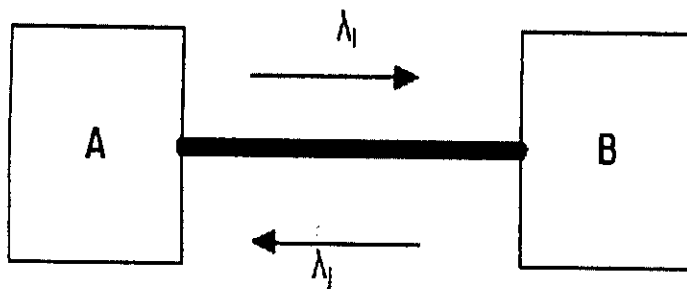
Figure 3.6: A bidirectional transmission system.
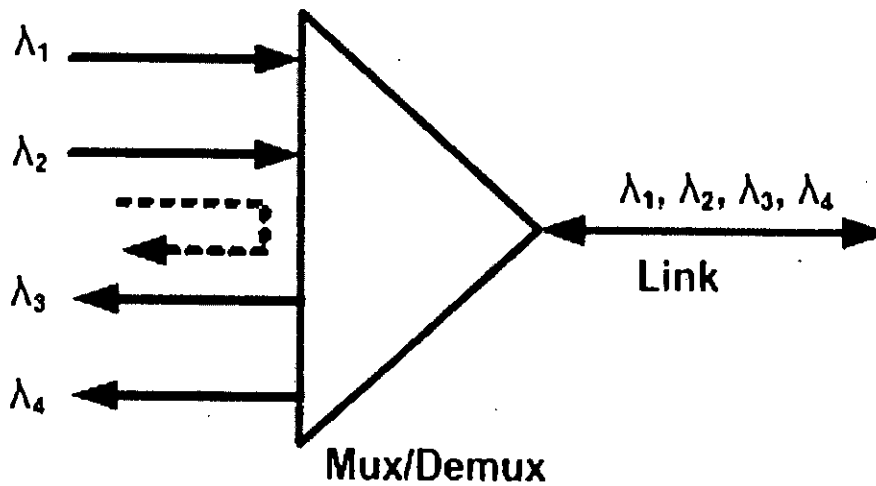
Figure 3.7: Separating the two directions in a bidirectional system using a WDM Mux/Demux. Crosstalk signal is shown by dashed line.

In fact, the reflected power into A may be larger than the signal power received from the other end B. The two directions can be separated at the ends by using a WDM Mux/Demux as shown in Figure 3.7. If a WDM Mux/Demux is used to handle both directions of transmissions, crosstalk can also arise, because a signal at a transmitted wavelength is reflected within the mux into a port that is used to receive signal from the other end, as in Figure 3.7.

3.3 Theory of In-Band Crosstalk

Figure 3.8 shows the schematic diagram of an N×N Arrayed Waveguide Grating (AWG) based multiplexer. To investigate the in-band crosstalk, each input port is assigned with a single wavelength λ_1. According to the diagram the signal from input port 1 is switched to the output port 3 as indicated by the solid line. But due to the imperfection of the AWG, a small amount of light from the input port 1 will be available to all other output ports. The solid and dashed arrows indicate the signal and the crosstalk propagation respectively. As seen in the figure the output light includes $N - 1$ crosstalk components. In brief, the signal light is mixed with

$N - 1$ same wavelength crosstalk light. The impact of $N - 1$ same wavelength
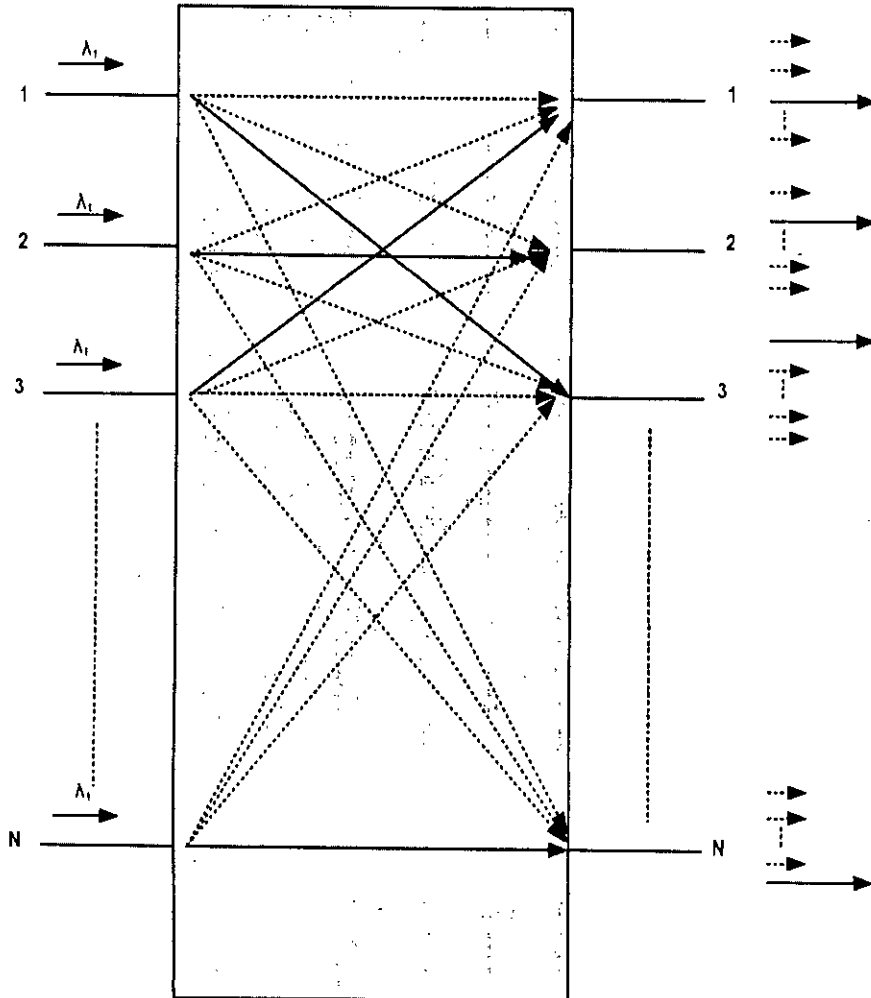
Figure 3.8: Schematic diagram of an N×N Arrayed Waveguide Grating (AWG) based multiplexer. Solid and dashed arrows indicate signal and crosstalk light propagation respectively.

crosstalk components can be analyzed as follows. Let us define the signal and crosstalk light as:

$$S_i(t) = \sqrt{2} E_i \sin(2\pi f_0 t + \phi_i(t)) \qquad \text{where}, i = 1 \text{ to } N$$

The subscript $i = 1$ denotes the signal and $i = 2$ to N denote the crosstalk components. f_0 is the laser oscillation frequency and $\phi_i(t)$ expresses the phase

noise of the laser. This includes the frequency drift of the laser. After the signal and $N-1$ crosstalk light are received by a photo detector at the destination node, the output photocurrent is given by [6],

$$i_p = E_1^2 + \sum_{i=2}^{N} 2E_1 E_i \cos(\phi_1(t) - \phi_i(t))$$
$$+ \sum_{i,j=2(i>j)}^{N} 2E_i E_j \cos(\phi_i(t) - \phi_j(t)) + \sum_{i=2}^{N} E_i^2 \qquad (3.1)$$

The first and last term are the optical power of the signal and crosstalk respectively. The second term is called signal-crosstalk beat noise. The third term is the crosstalk-crosstalk beat noise. The crosstalk-crosstalk beat noise is negligible compared to the signal-crosstalk beat noise [6].

The cosine function in the second term on the right hand side of equation 3.1 denotes the beat of the output current due to signal-crosstalk interference. If the whole noise power is inside the receiver bandwidth, the electrical noise power for each beat component is given by $2E_1^2 E_i^2$. The normalized noise power is obtained by adding the individual beat noise power and dividing the sum by the signal power. The result is,

$$\sigma_{RIN}^2 = \frac{1}{(E_1^2)^2} \sum_{i=2}^{N} 2E_1^2 E_i^2 = 2R_c(N-1) \qquad (3.2)$$

where, multiplexer crosstalk R_c is defined as the optical power ratio of each crosstalk component to the signal.

$$R_c = \frac{E_i^2}{E_1^2}$$

σ_{RIN}^2 is referred to as the relative intensity noise (RIN). Equation 3.6 is obtained for the continuous wave light. Actually, the crosstalk light as well as the signal is modulated. The signal-crosstalk beat occurs when the crosstalk channel is in the binary '1' state. If the probability of occurring binary '1' is 0.5, the noise power is

reduced by half. So the RIN of the signal crosstalk beat noise is given by,

$$\sigma_{RIN}^2 = R_c \times (N - 1) \tag{3.3}$$

Equation 3.3 shows that the RIN equals the sum of the relative optical powers of the crosstalk components.

The crosstalk-crosstalk beat noise can be analyzed as like as the signal-crosstalk beat noise. Each noise power is given by $2E_i^2 E_j^2$ and the beat occurs when the two participating components are in binary '1' state. So the power is reduced by three quarters. Accordingly the RIN of the crosstalk-crosstalk beat noise is given by,

$$\sigma_{RIN}^2 = \frac{1}{(E_1^2)^2} \sum_{i,j=2(i>j)}^{N} \frac{1}{4} 2E_i^2 E_j^2 = \frac{1}{4} R_c^2 (N - 1)(N - 2) \tag{3.4}$$

Equation 3.4 shows that the crosstalk-crosstalk beat noise is proportional to R_c^2 and seems smaller than the signal-crosstalk beat noise. So throughout our calculation we neglected the crosstalk-crosstalk beat noise.

3.3.1 Analysis of In-Band Crosstalk for Multiwavelength Optical Cross-Connects.

A typical structure of optical cross-connect(OXC) is shown in Figure 3.9. The OXC consists of a total of N optical demultiplexers, M optical switches, and N multiplexers. Each of the input fibers to an optical demultiplexers contains M different wavelengths. The optical demultiplexers spatially separates the incoming wavelengths into M paths. Each of these paths passes through an optical switch before they are combined with the outputs from the other $M - 1$ optical switches.

Assuming the OXC is fully loaded, each signal passing through the OXC will be interfered by $M + N - 2$ homodyne crosstalk contributions, $N - 1$ of which are leaked by the optical switch, and the other $M - 1$ are leaked by the demultiplexer/multiplexer pair. For facilitating the description, we now consider the signal with wavelength 1 in input fiber 1, noted as λ_{11} as the main signal.
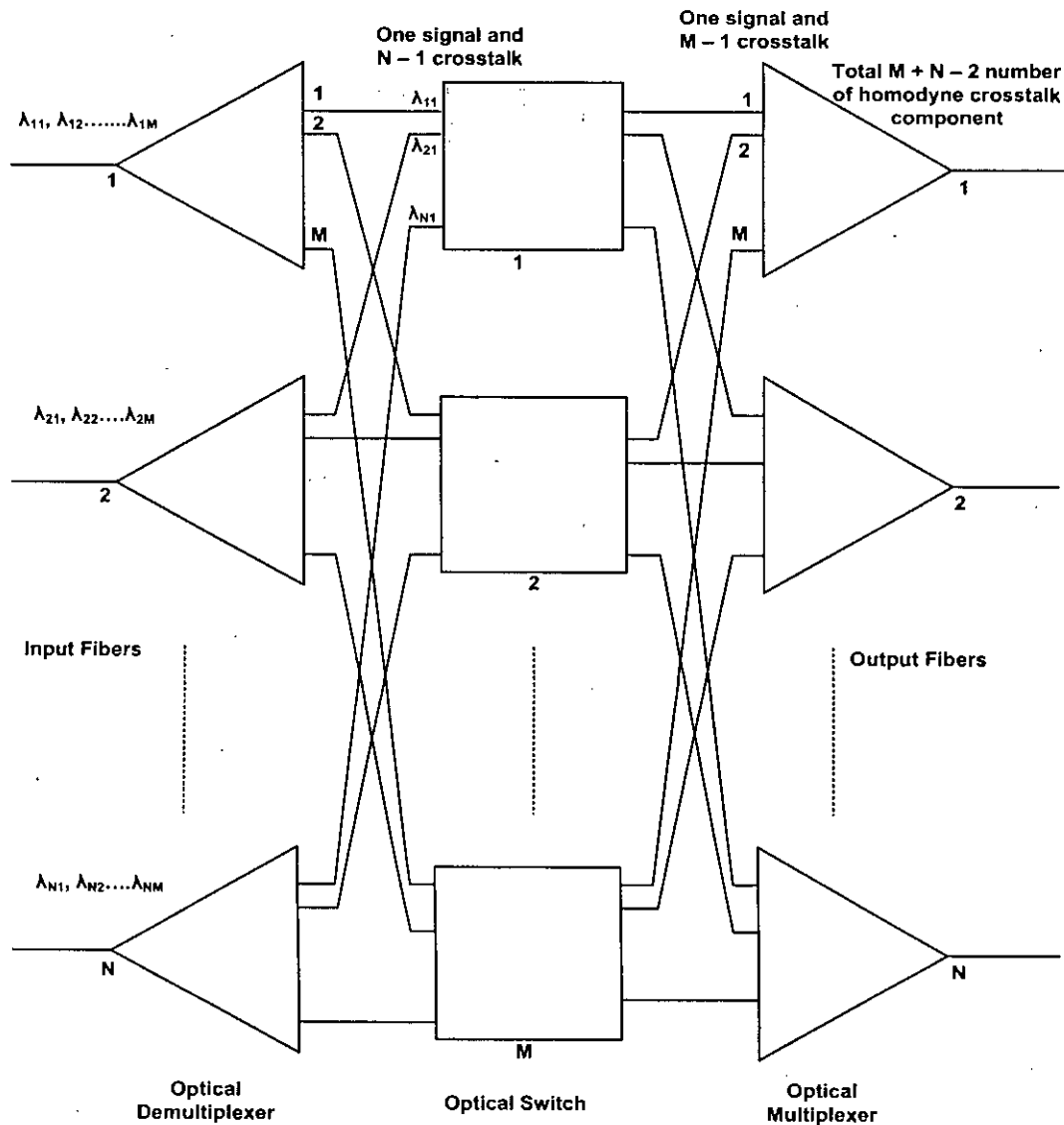
Figure 3.9: Typical structure of an OXC having N input and output ports and M wavelengths at each port.

The main signal λ_{11} will be interfered by $N-1$ crosstalk contributions leaked from the $N-1$ signals with wavelength 1 ($\lambda_{21}, \lambda_{31}, \ldots \lambda_{N1}$) in the other $N-1$ input fibers, when passing through the optical switch 1, because of the non ideal crosstalk

specification of optical switches. The $N - 1$ crosstalk contributions can be treated as generated by different lasers and they are phase incorrelated with λ_{11}, and with each other. Similarly, when each signal with wavelength 1 is demultiplexed into one path, there will be a fraction of it in each other $M - 1$ outputs of the corresponding demultiplexer because of the non ideal crosstalk specification of optical demultiplexers. After passing through the optical switches, the main signal is multiplexed with $M - 1$ signals with different wavelengths. At the same time, the $M - 1$ crosstalk contributions of wavelength 1 in the $M - 1$ paths are combined with the main signal though isolated again by the optical multiplexer. These $M - 1$ crosstalk contributions can be leaked from signal with wavelength 1 in all the N input fibers. Some of them can be leaked from λ_{11} , i.e., the main signal itself. Number of contributions leaked from λ_{11} is the coherent part of the crosstalk. But here we assume that all the $M - 1$ crosstalk components are incoherent.

The expression of photocurrent, i_p can be given as:

$$i_p = E_1^2 + \sum_{i=2}^{M+N-1} 2E_1 E_i \cos(\phi_1(t) - \phi_i(t))$$
$$+ \sum_{i,j=2(i>j)}^{M+N-1} 2E_i E_j \cos(\phi_i(t) - \phi_j(t)) + \sum_{i=2}^{M+N-1} E_i^2 \qquad (3.5)$$

The expression of relative intensity noise caused by the beat noise of the signal and $M + N - 2$ homodyne crosstalk components can be given as,

$$\sigma_{RIN}^2 = R_c \times (M + N - 2) \qquad (3.6)$$

3.4 Theory of Inter-Band Crosstalk

The received baseband digital signal $b(t)$ in time domain is given by the well known rectangular function,

$$b(t) = A \; rect(\frac{t}{T_b})$$

where, $A = \sqrt{2Pr}$ is the amplitude of the signal, Pr being the received power, and T_b is the bit period.
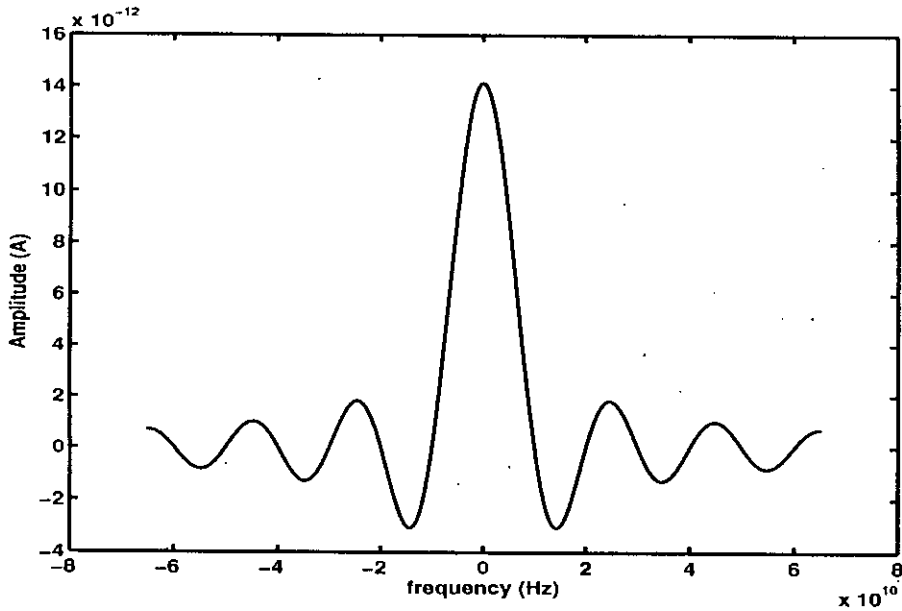
Figure 3.10: A binary '1' in frequency domain. $Pr = -20\text{dBm}$, $B = 10^9 Hz$.

In frequency domain, this digital bit becomes sinc function as given by,

$$B(f) = \sqrt{2Pr}\ T_b \frac{sin(\pi f T_b)}{(\pi f T_b)}$$

Figure 3.10 shows the spectrum of a baseband binary '1'. Clearly, the spectrum of the digital signal extends over the range $-\infty < f < \infty$. The side lobes of the spectrum cause crosstalk with the adjacent signal.

In Figure 3.9 we can see that at the output multiplexer, M wavelengths are multiplexed together. Here adjacent $M - 1$ wavelengths cause inter-band crosstalk. The inter-band crosstalk can better be understood by observing the Figure 3.11. We can see that the side lobes from the adjacent channels are causing the inter channel crosstalk. This crosstalk cannot be eliminated by the receiver filtering because it falls within the receiver bandwidth coming from the adjacent channel frequencies. The variance of noise power induced by inter-band crosstalk as shown
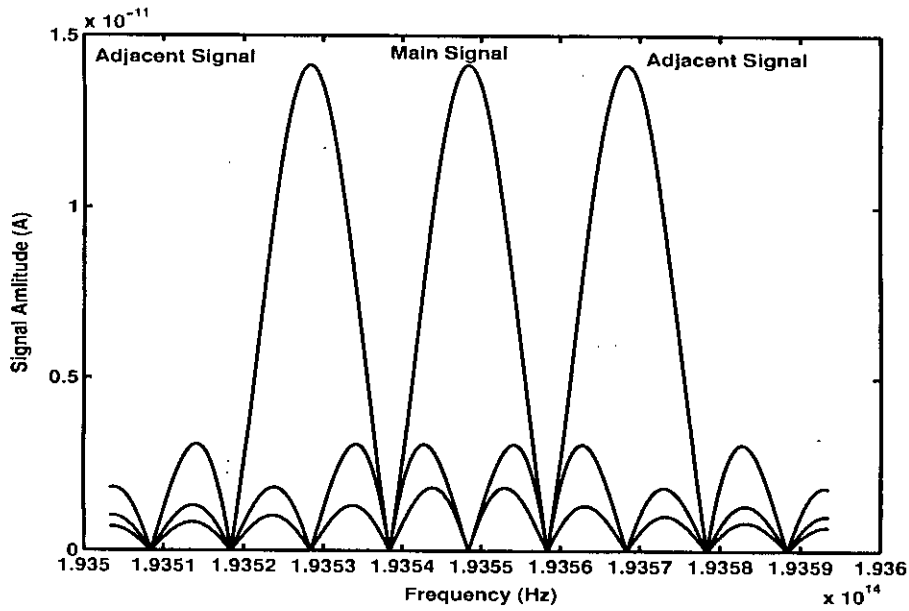
Figure 3.11: Accumulation of inter-band crosstalk.

in Figure 3.11 can be given as,

$$\sigma^2_{inter} = \sum_{i=1(f_i \neq f_s)}^{M} \int_{f_s-B/2}^{f_s+B/2} (\sqrt{2Pr}\, T_b)^2 \left| \frac{\sin(\pi(f - f_i)T_b)}{\pi(f - f_i)T_b} \right|^2 df \qquad (3.7)$$

where,

f_s = Signal frequency,

f_i = Frequency of the crosstalk signals,

B = Receiver bandwidth,

Pr = Received power for the binary '1',

T_b = Bit period,

f = Frequency, and

M = No of wavelengths.
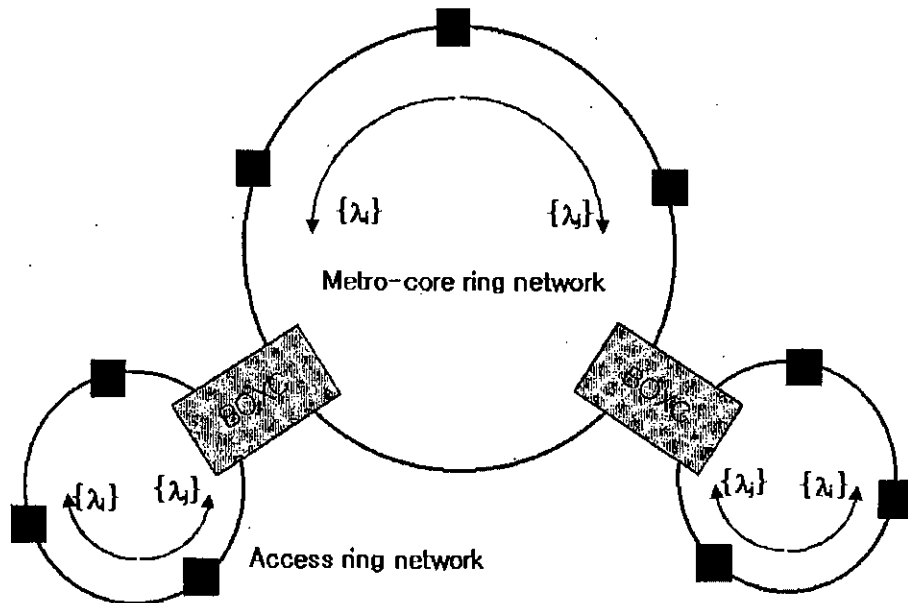
Figure 3.12: Schematic diagram of bidirectional WDM ring networks interconnected by bidirectional OXCs. In each ring network, two different sets of wavelength channels propagate in opposite direction.

3.5 Bidirectional Optical Cross-Connect

Figure 3.12 shows a schematic diagram of a feasible metropolitan area network (MAN) composed of bidirectional WDM ring networks (BWRNs), in which small access ring networks are connected to a big metro-core ring network through the use of BOXCs. Figure 3.13 shows the schematic diagram of a BOXC. In a BWRN in Figure 3.12, two different sets of wavelengths propagate in different directions. We may use two separate wavelength bands for their respective directions or we may adopt the interleaved wavelength scheme in which two sets of wavelength channels are interleaved to each other.

Figure 3.13 depicts the configuration of BOXC, interconnecting two single fiber BWRNs. In the upper and lower ring of Figure 3.13, we assume that $\lambda_1, \lambda_1, \ldots \lambda_{M/2-1}$ and $\lambda_{M/2+1}, \lambda_{M/2+2}, \ldots \lambda_{M-1}$ propagate in opposite directions. The signals $\lambda_1, \lambda_1, \ldots \lambda_{M/2-1}$ launched into port $M/2$ and port M from the upper and lower BWRNs respectively, are demultiplexed into the fold back optical paths on the right side of the AWG router and encounter the tunable FBGs. Depending
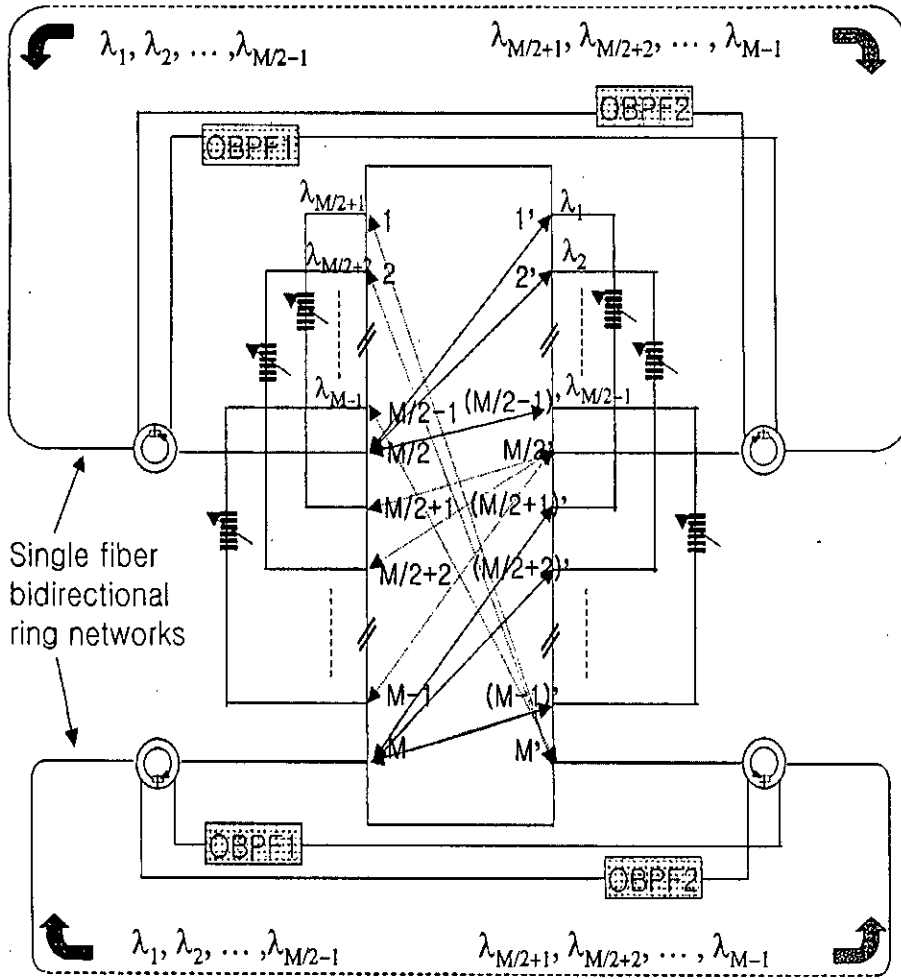
Figure 3.13: Schematic diagram of a typical BOXC.

on the center wavelength of each FBG, each wavelength will pass through or be reflected back by the FBG. The reflected signal will be coupled back to the ports from which they come and remain in the same BWRN passing through two four-port circulators and an optical band pass filter (OBPF), which is called as the bar state. On the contrary, the through passing signal will be coupled into the other ports and move to the other BWRNs, which corresponds to a cross state. Similarly for the wavelength channels of $\lambda_{M/2+1}, \lambda_{M/2+2}, \ldots \lambda_{M-1}$ launched into port $(M/2)'$ and port M', we can achieve the same independent switching between the upper and the lower rings by tuning the FBGs in the fold back path on the left side. The OBPFs in the BOXC suppress unwanted backscattered signals. The source of the

backscattering are the Rayleigh scattering in the fiber and the reflection in the connectors. The pass band of OBPF1 covers $\lambda_1, \lambda_1, \ldots \lambda_{M/2-1}$ and that of OBPF2 covers $\lambda_{M/2+1}, \lambda_{M/2+2}, \ldots \lambda_{M-1}$. Backscattering induced RIN is a serious problem in BOXC. Let us consider the wavelength λ_i, which is switched from upper BWRN to the lower BWRN. The backscattered λ_i in the lower BWRN will reenter the BOXC and switch back to the upper BWRN. The backscattering induced RIN for a BOXC can be given [15] as,

$$\sigma_{bs}^2 = \frac{1}{2} R_{bs}^2 i_p^2 \tag{3.8}$$

where, R_{bs} is the equivalent reflectivity of backscattering. i_p is given by equation 3.5 which includes the effect of number of channel, N and number of wavlenghths per channel, M. For the BWRN considered above N = 2.

3.6 Expression for Bit Error Rate (BER)
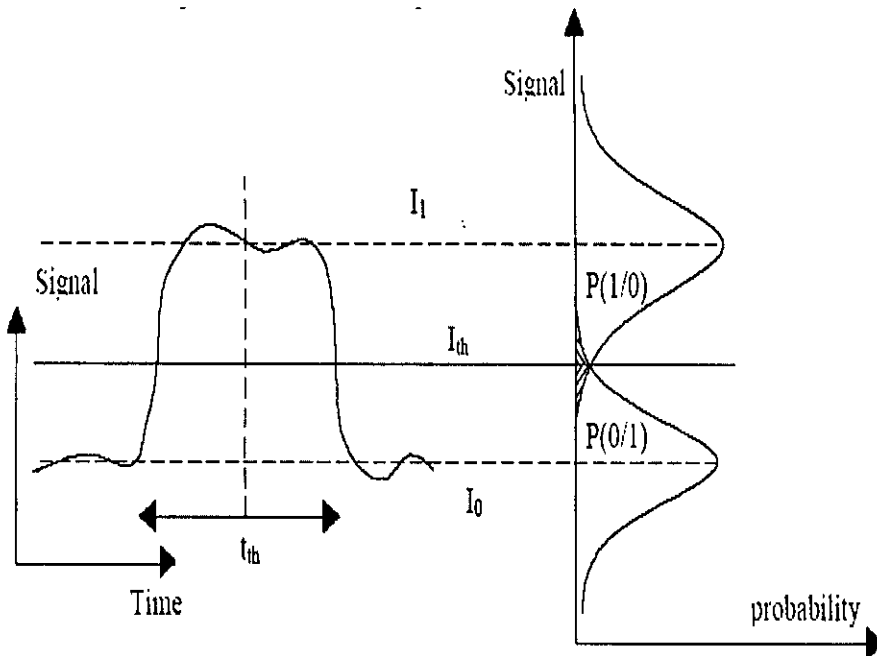
Figure 3.14: Electrical signal after photo detection and conditional gaussian densities of probability.

The goal of the photo receiver is to sample the signal at the decision time t_{th} and to make a decision concerning its value, as shown in Figure 3.14.

The decision circuit compares the received sampled value to the threshold value I_{th} and forces the bit value to 1 when $I > I_{th}$ and to 0 when $I < I_{th}$. An error occurs when $I > I_{th}$, whereas the value of the bit symbol is 0 and vice versa. We can define the error probability as:

$$\text{Error probability} = p(1) \times p(0|1) + p(0) \times p(1|0)$$

where $p(1)$ and $p(0)$ are the probabilities of transmitting a symbol 1 and 0 respectively. $p(0|1)$ and $p(1|0)$ are the probabilities of incorrect identification. Assuming the same number of symbols 0 and 1, we have:

$$p(1) = p(0) = \frac{1}{2}$$

$$\text{Error Probability} = \frac{1}{2}\Big[p(0|1) \times p(1|0)\Big]$$

Assuming that the distribution of the different sources of noise is gaussian, we can deduce that the distribution of noise on symbols 1 and 0 is also gaussian and can be defined by their variances σ_1^2 and σ_0^2. It is then possible to define the conditional probabilities $p(1|0)$ and $p(0|1)$ [17] as:

$$p(0|1) = \frac{1}{\sigma_1\sqrt{2\pi}} \int_{-\infty}^{I_{th}} e^{-\frac{(I-I_1)^2}{2\sigma_1^2}} dI = \frac{1}{2} \, erfc\left(\frac{I_1 - I_{th}}{\sigma_1\sqrt{2}}\right)$$

$$p(1|0) = \frac{1}{\sigma_0\sqrt{2\pi}} \int_{I_{th}}^{+\infty} e^{-\frac{(I-I_0)^2}{2\sigma_0^2}} dI = \frac{1}{2} \, erfc\left(\frac{I_{th} - I_0}{\sigma_0\sqrt{2}}\right)$$

where erfc is the complementary error function defined by,

$$erfc(x) = \frac{2}{\sqrt{\pi}} \int_{x}^{+\infty} e^{-y^2} dy$$

I_1 is the photocurrent for binary '1' and I_0 is the photocurrent for binary '0'. The bit error rate can then be expressed as:

$$BER = \frac{1}{4} \times \left[erfc\left(\frac{I_1 - I_{th}}{\sigma_1\sqrt{2\pi}}\right) + erfc\left(\frac{I_{th} - I_0}{\sigma_0\sqrt{2\pi}}\right) \right].$$

This rate depends on the decision threshold I_{th}. Generally, the decision threshold is chosen to minimize the bit error rate. In our analysis, fixed decision threshold is used,

$$I_{th} = \frac{I_1}{2}$$

Assuming infinite extinction ratio, $I_0 = 0$ we get,

$$BER = \frac{1}{4} \times \left[erfc\left(\frac{I_1}{2\sqrt{2}\sigma_1}\right) + erfc\left(\frac{I_1}{2\sqrt{2}\sigma_0}\right)\right] \tag{3.9}$$

3.7 Impact of Crosstalk on BER

The general formula for the Bit Error Rate (BER) for Intensity Modulation-Direct Detection (IM-DD) is given by,

$$BER = \frac{1}{4} \, erfc\left(\frac{i_p}{2\sqrt{2}\sigma_1}\right) + \frac{1}{4} \, erfc\left(\frac{i_p}{2\sqrt{2}\sigma_0}\right) \tag{3.10}$$

i_p is the photocurrent when the signal is in binary '1' state. This corresponds to optical power. σ_0 denotes the receiver noise which exists in the absence of crosstalk. The first and second terms are the bit error rate when the signals are binary '1' and binary '0' respectively. It is assumed for simplicity that the receiver noise is mainly due to the thermal noise and there is no difference in '1' and '0' state. Thermal noise of the receiver is given by,

$$\sigma_0^2 = \frac{4kTB}{R_L} \tag{3.11}$$

where,

k = Boltzman constant,

T = Room temperature in degree Kelvin,

B = Receiver Bandwidth in Hz, and

R_L = Resistance of the load bus in ohm.

3.7.1 BER in Absence of Crosstalk

When there is no crosstalk BER is affected only by the thermal noise of the receiver as stated in section 3.7. We also assumed that the thermal noise is same for binary

'1' and '0' state, i.e., $\sigma_1 = \sigma_0$. In the absence of crosstalk the photocurrent i_p, assuming unity responsivity is given by,

$$i_p = E_1^2 \tag{3.12}$$

The equation of BER is given by,

$$BER = \frac{1}{4} \, erfc\left(\frac{i_p}{2\sqrt{2}\sigma_0}\right) + \frac{1}{4} \, erfc\left(\frac{i_p}{2\sqrt{2}\sigma_0}\right) = \frac{1}{2} \, erfc\left(\frac{i_p}{2\sqrt{2}\sigma_0}\right) \tag{3.13}$$

3.7.2 BER due to In-Band Crosstalk

In-Band crosstalk is analyzed in section 3.3. For the OXC shown in Figure 3.8 which uses one wavelength for each of N input ports, i_p is given by equation 3.1 and for the OXC shown in Figure 3.9, which uses M wavelengths for each of N input ports, i_p is given by equation 3.5.

It is assumed here that the beat noise has an approximately Gaussian probability density distribution, which is true according to the central limit theorem which tells that when the number of channel increases, the probability distribution of beat noise becomes the Gaussian distribution. Therefore, the total noise in the presence of crosstalk is simply given by the sum of the beat noise and the receiver noise.

$$\sigma_1 = \sqrt{\sigma_0^2 + \sigma_{intra}^2} \tag{3.14}$$

where, σ_0^2 is given by the equation 3.11. For the OXC shown in Figure 3.8 which uses one wavelength for each of N input ports, σ_{intra}^2 is given by,

$$\sigma_{intra}^2 = R_c \times (N-1) \times i_p^2 \tag{3.15}$$

For the OXC shown in Figure 3.9, which uses M wavelengths for each of N input ports, σ_{intra}^2 is given by,

$$\sigma_{intra}^2 = R_c \times (M+N-2) \times i_p^2 \tag{3.16}$$

3.7.3 BER due to Inter-Band Crosstalk

Inter-band crosstalk is discussed in section 3.4. According to the central limit theorem, the inter-band crosstalk also assumes the gaussian distribution. To investigate the effect of inter-band crosstalk, the variance of noise power due to inter-band crosstalk as found by equation 3.7 is added along with the thermal noise of the receiver to get the receiver noise at binary '1' state. Therefore, the receiver noise in presence of inter-band crosstalk is given by,

$$\sigma_1 = \sqrt{\sigma_0^2 + \sigma_{inter}^2} \qquad (3.17)$$

where, σ_0^2 is given by the equation 3.11 and σ_{inter}^2 is the variance of noise power due to inter-band crosstalk and is given by the equation 3.7.

Photocurrent, i_p in the expression of BER of equation 3.10 is given by the equation 3.12 as we are considering only the effect of inter-band crosstalk.

3.7.4 BER due to In-Band and Inter-Band Crosstalk

If in-band and inter-band crosstalk are considered together then the variance of noise power in binary '1' state, σ_1 is given by,

$$\sigma_1 = \sqrt{\sigma_0^2 + \sigma_{intra}^2 + \sigma_{inter}^2} \qquad (3.18)$$

where, σ_0^2 is given by the equation 3.11, σ_{intra}^2 is given by the equation 3.16 and σ_{inter}^2 is given by the equation 3.7.

Photocurrent, i_p in the expression of BER of equation 3.10 is given by the equation 3.5.

3.7.5 BER due to Backscattering Induced Crosstalk

Backscattering that occurs in BOXC is discussed in section 3.5 and the backscattering induced RIN is given by equation 3.8. The crosstalk due to backscattering is considered again to be gaussian in nature and this crosstalk is directly added with inter-band and in-band crosstalk to get the overall crosstalk. In equation 3.10 to observe the BER, photocurrent, i_p is used from the equation 3.5 and the

receiver noise σ_1 in binary '1' state is given by,

$$\sigma_1 = \sqrt{\sigma_0^2 + \sigma_{intra}^2 + \sigma_{inter}^2 + \sigma_{bs}^2} \qquad (3.19)$$

where, σ_0^2 is given by the equation 3.11, σ_{intra}^2 is given by the equation 3.16, σ_{inter}^2 is given by the equation 3.7 and σ_{bs}^2 is given by the equation 3.8.

3.8 Summary

Theoretical study of different types of crosstalks present in unidirectional and bidirection OXCs is given in this chapter. The leakage of crosstalk signal in multiplexers/demultiplexera and switches is explained. The propagation of different crosstalks in unidirectional and bidirectional OXCs is studied. Analytical expression of these crosstalks are developed and the expression of BER is modified including the effect of these crosstalks.

Chapter 4

Results and Discussion

In this chapter, the BER performance and power penalty due to the presence of different types of crosstalk in OXCs of a WDM system are investigated. The simulation results and brief discussion on those results are also presented.

4.1 Impact of In-Band Crosstalk

The detail analysis of in-band crosstalk is described in section 3.3. Figure 3.9 shows a typical OXC and the in-band crosstalk induced RIN due to this OXC is given by equation 3.6. The effect of this RIN on BER is described in section 3.7.2. To observe the BER performance, we simulated equation 3.10, incorporating the in-band crosstalk induced RIN into this equation. To evaluate the expression of σ_0 as given by equation 3.11, we assumed T = 300K, k = 1.38×10^{-23}, B = 10^9 Hz, and $R_L = 50\Omega$.

Figure 4.1 gives the comparative plots of BER against the received power for different number of channels and different number of wavelengths per channel. In each plot of Figure 4.1 [(a)-(d)], the number of channels, N is varied from 4 to 16 with the increment of 4 channels per step and it is found that the BER increases significantly with the increase of N. Different no. of wavelengths per channel, M is used for each plot of Figure 4.1 [(a)-(d)] to observe the effect of M on BER. It is also found from the plot that the BER increases with the increase of number of wavelengths per channel. Table 4.1 describes the dependancy of BER on the
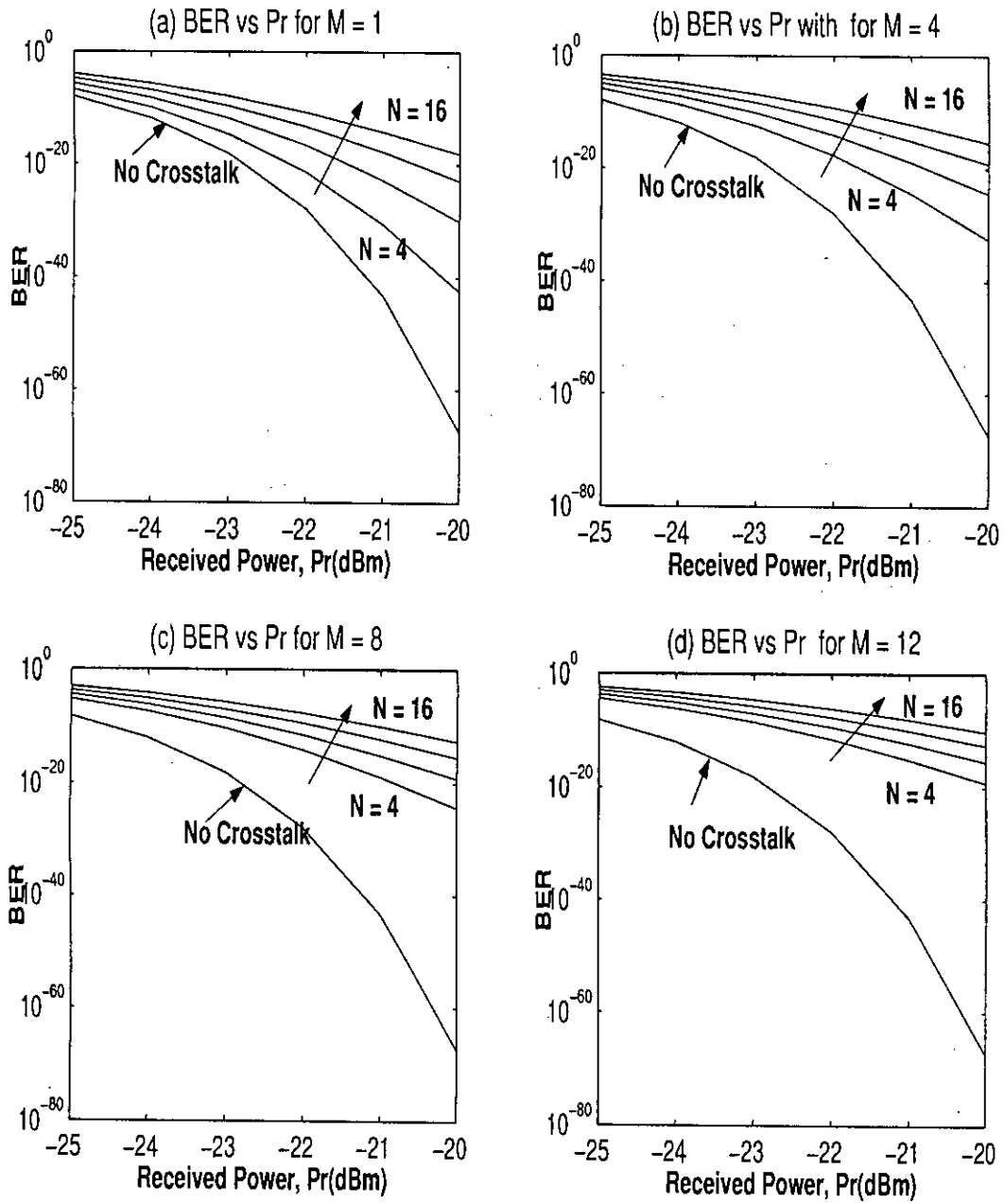
Figure 4.1: BER performance in presence of in-band crosstalk with varying number of channels. Dependance of number of wavelengths per channel is also presented. Component crosstalk, $R_c = -40$dB is assumed.

number of channels and number of wavelengths per channel.

Figure 4.2 shows the plot of power penalty against the number of channels due to the in-band crosstalk induced RIN in a typical OXC, shown in Figure 3.9. This plot is found from the data obtained from the plots of Figure 4.1. The data for the calculation of power penalty is taken for a standard BER of 10^{-9}. This plot shows that the power penalty increases almost linearly with the increase in number of channels.
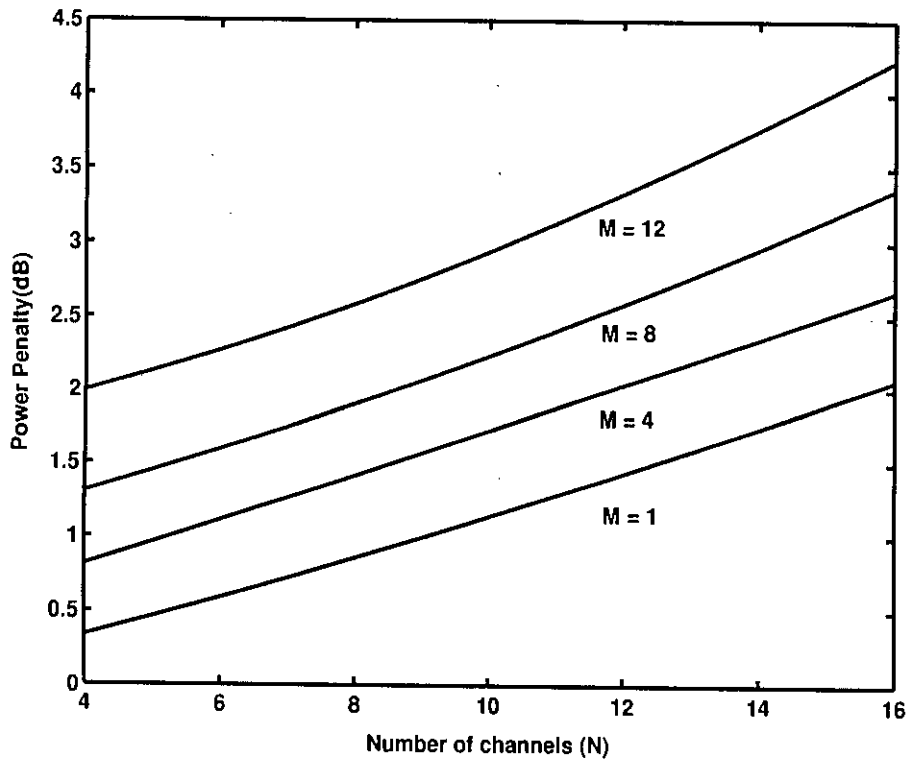
Figure 4.2: Power penalty as a function of number of channels for different number of wavelengths per channel. Power penalty is plotted to get an overall BER of 10^{-9}. The data is obtained from Figure 4.1.

We have also simulated the effect of number of wavelengths per channel on power penalty and the results are shown in Figure 4.2. We have got an upward shift of power penalty against number of channels for an increase in number of wavelengths per channel which indicates that the power penalty also increases with the increase in number of wavelengths per channel. Table 4.2 describes the dependancy of power penalty on the number of channels and number of wavelengths per channel.
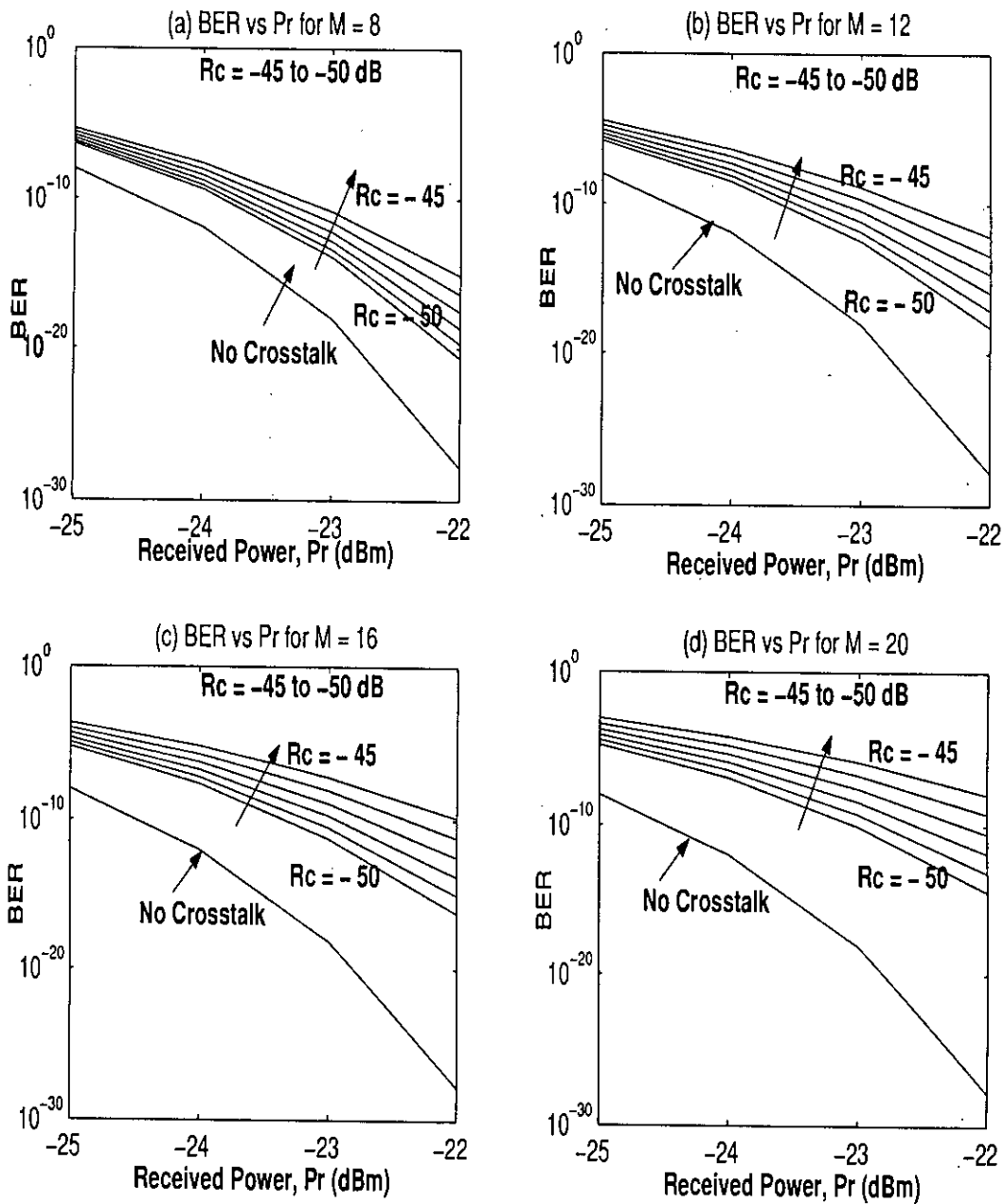
Figure 4.3: BER performance due to in-band crosstalk for varying component crosstalk. Dependance of the BER performance on number of wavelengths per channel is also presented. $N = 4$ is assumed for this simulation.

Figure 4.3 gives the plot of BER performance due to in-band crosstalk induced noise with the variation of component crosstalk. Component crosstalk is varied from -45 dB to -50 dB as shown in figure. Again, the number of wavelength is

varied in each case of Figure 4.3 [(a)-(d)]. With the knowledge of theoretical study, we know that the BER will increase with the increase of component crosstalk and it is found through our simulation result. Dependance of BER on the number of wavelengths per channel is also obtained in this figure. Table 4.1 describes the effect of component crosstalk and number of wavelengths per channel on the BER performance.
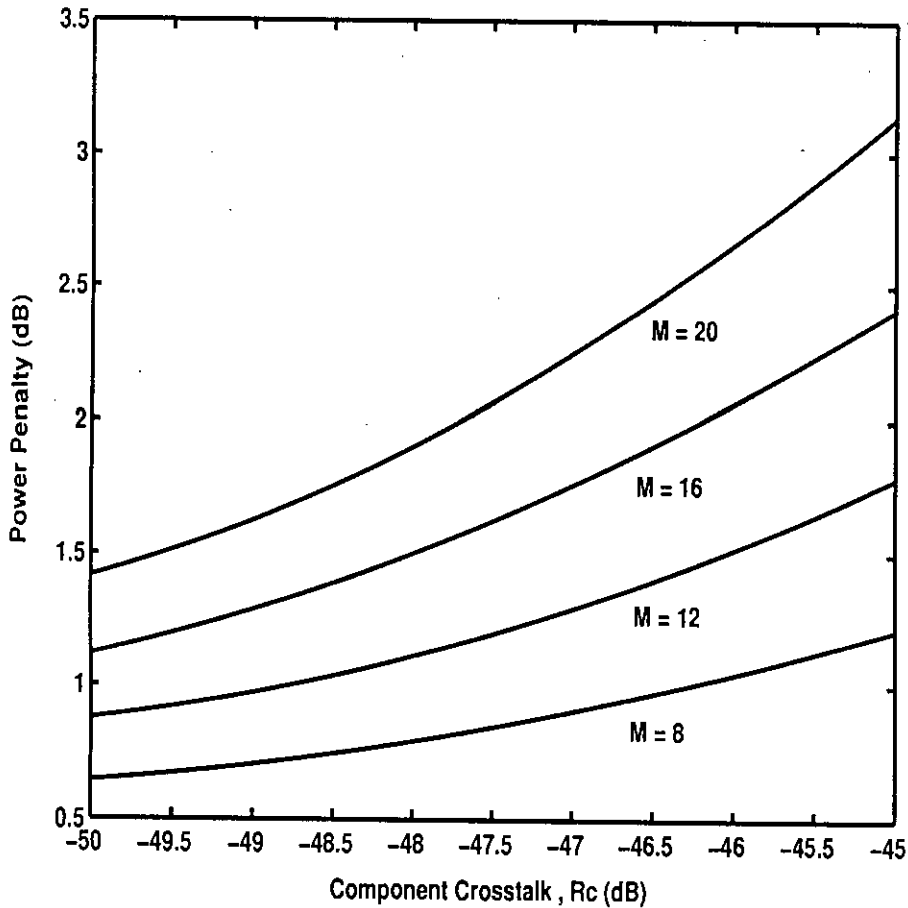
Figure 4.4: Power penalty as a function of component crosstalk due to in-band crosstalk. Dependance of this power penalty on different number of wavelengths per channel is also presented. Power penalty is plotted to get an overall BER of 10^{-9}. Data is obtained from the plot of Figure 4.3.

The power penalty against the component crosstalk is presented in Figure 4.4. This power penalty is plotted for a BER of 10^{-9} and the required data is found from the above mentioned analysis. It is found from the plot that the power penalty

Table 4.1: BER performance due to in-band crosstalk.

Pr (dBm)	R_c (dB)	M	N	BER
-22	-40	8	4	10^{-13}
			12	10^{-9}
		12	4	10^{-11}
			12	10^{-8}
	-45	8	4	10^{-15}
		12	4	10^{-12}

Table 4.2: Power penalty due to in-band crosstalk.

N	R_c (dB)	M	PP (dB)
4	-40	8	1.3
		12	2
	-45	8	1.21
		12	1.78

increases with the increase of component crosstalk. The increase in number of wavelengths per channel also increases the power penalty, giving an upward shift of the power penalty in the plot against number of channels. Table 4.2 demonstrates the effect of component crosstalk and number of wavelengths per channel on power penalty.

The comparative analysis of BER and power penalty and is given in Table 4.1 and Table 4.2 with the variation of different system parameters.

4.2 Impact of Inter-Band Crosstalk

The theory of inter-band crosstalk is described in section 3.4 and is given by equation 3.17. The simulation result of equation 3.17 gives the crosstalk as a function of channel separation as shown in Figure 4.5. The number of wavelengths per chan-
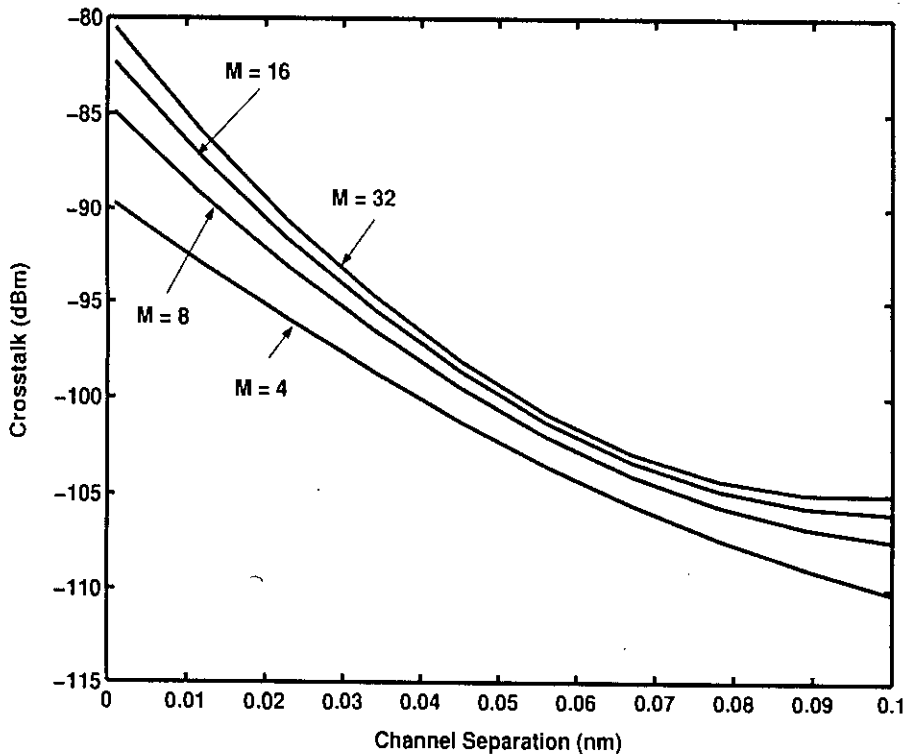
Figure 4.5: Inter-band crosstalk as a function of channel separation for different number of wavelengths per channel.
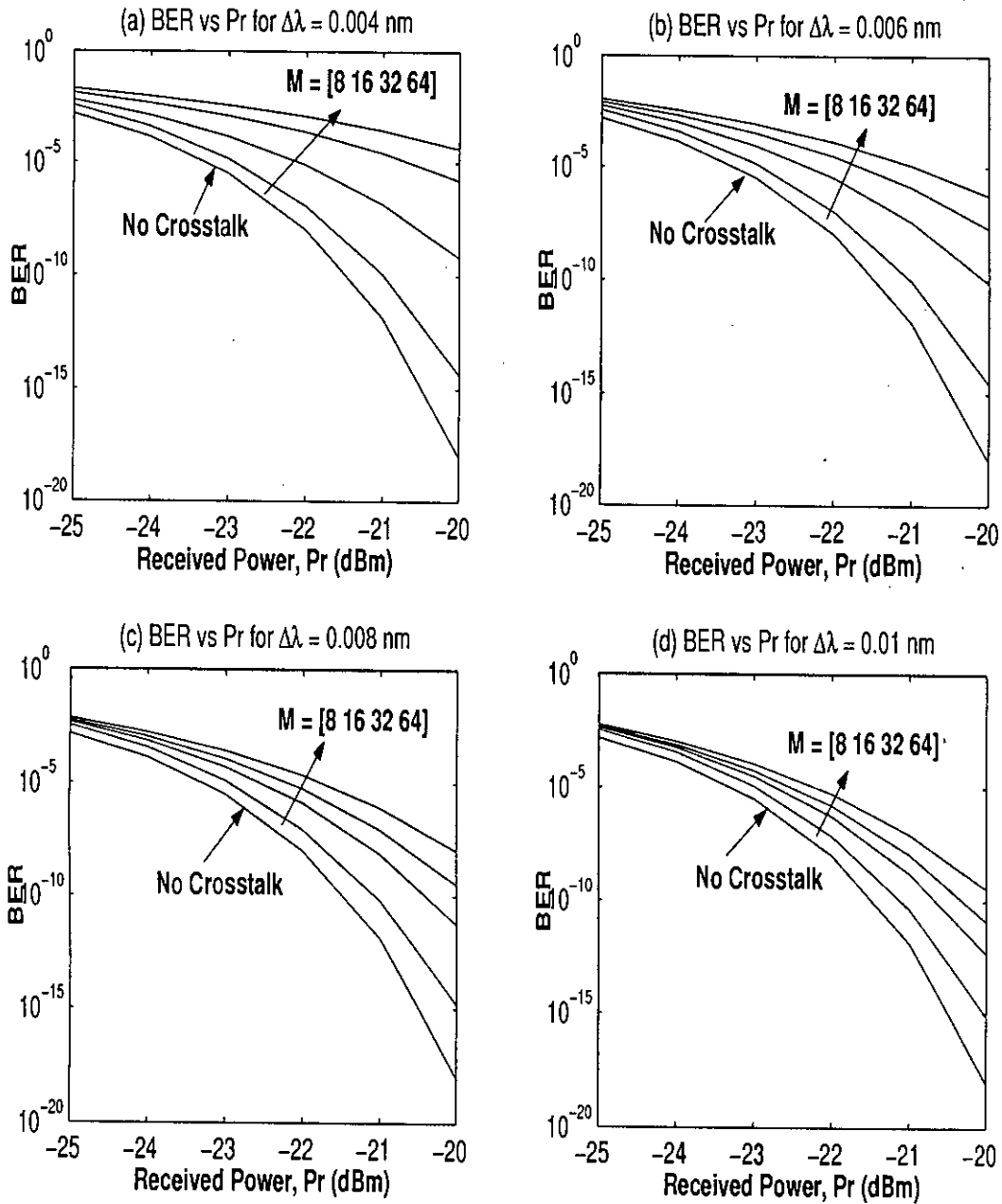
Figure 4.6: BER performance due to inter-band crosstalk with varying number of wavelengths and different channel separations.

nel is varied to observe its effect on inter-band crosstalk. It is clear from the plot that when the channel separation is decreased, crosstalk becomes severe. Rapid increase in traffic demand leads us to decrease the channel separation. Therefore

inter-band crosstalk should be taken into account as the channel separation decreases. This crosstalk is severe in the sense that it can not be eliminated by the filtering arrangement in the receiver as it falls within the receiver bandwidth. Table 4.3 gives the comparative statistics of crosstalk with the variation of channel separation and number of wavelengths.

The crosstalk found in Figure 4.5 is incorporated in equation 3.10 to observe the BER performance in presence of inter-band crosstalk. To observe solely the effect of inter-band crosstalk on the BER performance, we assumed that crosstalk other than the inter-band crosstalk is absent in the current study. The simulation result is plotted in Figure 4.6 [(a)-(d)]. The number of wavelengths was varied from 8 to 20 with an increment of 4 per step and the effect is observed for each plot.
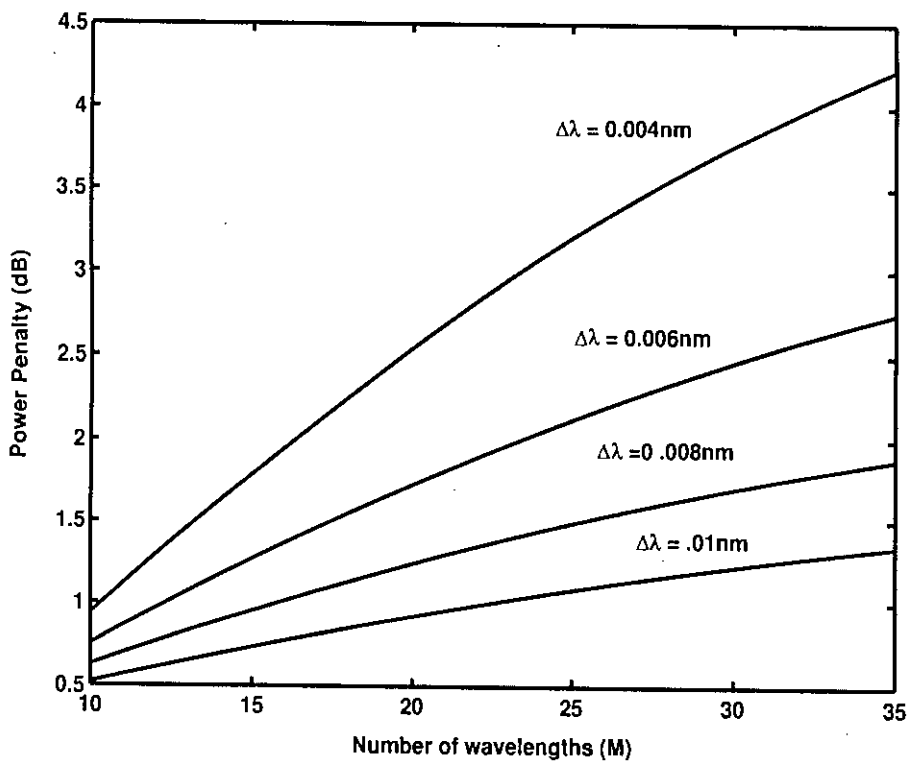

Figure 4.7: Power penalty due to inter-band crosstalk against the number of wavelengths. Dependance of this power penalty on channel separation is also presented. Power penalty is plotted for an overall BER of 10^{-9}.

Table 4.3: Crosstalk due to inter-band crosstalk.

Δλ (nm)	M	Crosstalk (dBm)
0.02	8	− 85.5
	16	− 83.0
0.1	8	− 107.5
	16	− 106

It is found that BER increases with the increase of number of wavelengths per channel due to inter-band crosstalk induced noise. In figure 4.6 [(a)-(d)], channel separation is varied to observe the BER performance dependance on channel separation. We have found that the BER decreases from (a) to (d) with the increase in channel separation. Dependance of BER performance on channel separation and number of wavelengths per channel is given in Table 4.4.

In Figure 4.7, power penalty is plotted against the number of wavelengths per channel. This plot is found from the data obtained from the plot of Figure 4.6 [(a)-(d)] to obtain a BER of 10^{-9}. In the same plot, we have also observed the effect of channel separation on power penalty. We found that power penalty versus number of wavelengths per channel curve shifts upward for the decrease in channel separation signifying that power penalty increases with the decrease in channel separation. Table 4.5 gives the relative values of power penalty depending on the channel separation and number of wavelengths per channel. We see that a power penalty of 4.2 dBm is possible for a channel separation of 0.004 nm. So inter-band crosstalk cannot be neglected as mentioned by some literatures [4] - [9].

Table 4.4: BER performance due to inter-band crosstalk.

Pr (dBm)	Δλ (nm)	M	BER
−20	0.004	8	10^{-14}
		16	10^{-9}
	0.01	8	10^{-15}
		16	10^{-12}

Table 4.5: Power penalty due to inter-band crosstalk.

M	Δλ (nm)	PP (dB)
16	0.004	1.9
	0.01	0.57
32	0.004	4.2
	0.01	1.3

4.3 Impact of Backscattering Induced Crosstalk

A typical bidirectional optical cross-connect is described in section 3.5 and the theory of backscattering induced crosstalk due to bidirectional OXCs is described in details in the same section. It was concluded that the backscattering induced crosstalk is a serious problem for BOXCs. We incorporated the backscattering
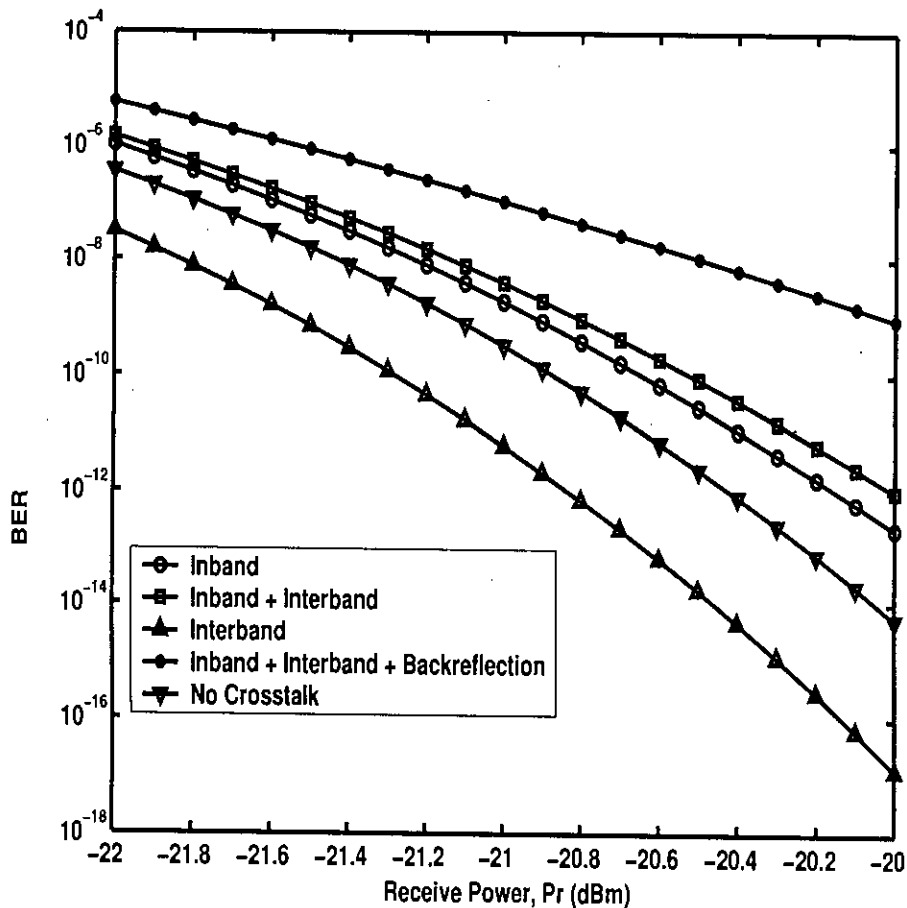
Figure 4.8: BER performance of different types of crosstalk in unidirectional and bidirectional OXCs. Number of channels, number of wavelengths per channel, channel separation, backscattering coefficient and component crosstalk are considered to be fixed. N = 4, M = 4, $\Delta\lambda$=0.006nm, $R_{bs} = -25$ dB and $R_c = -40$dB.

induced noise as given by equation 3.8 into the bit error rate expression in equation 3.10 as described in section 3.7.5. In the present analysis, we incorporated in-band crosstalk, inter-band crosstalk and the backscattering induced crosstalk to observe the effect of overall BER performance of a BOXC.
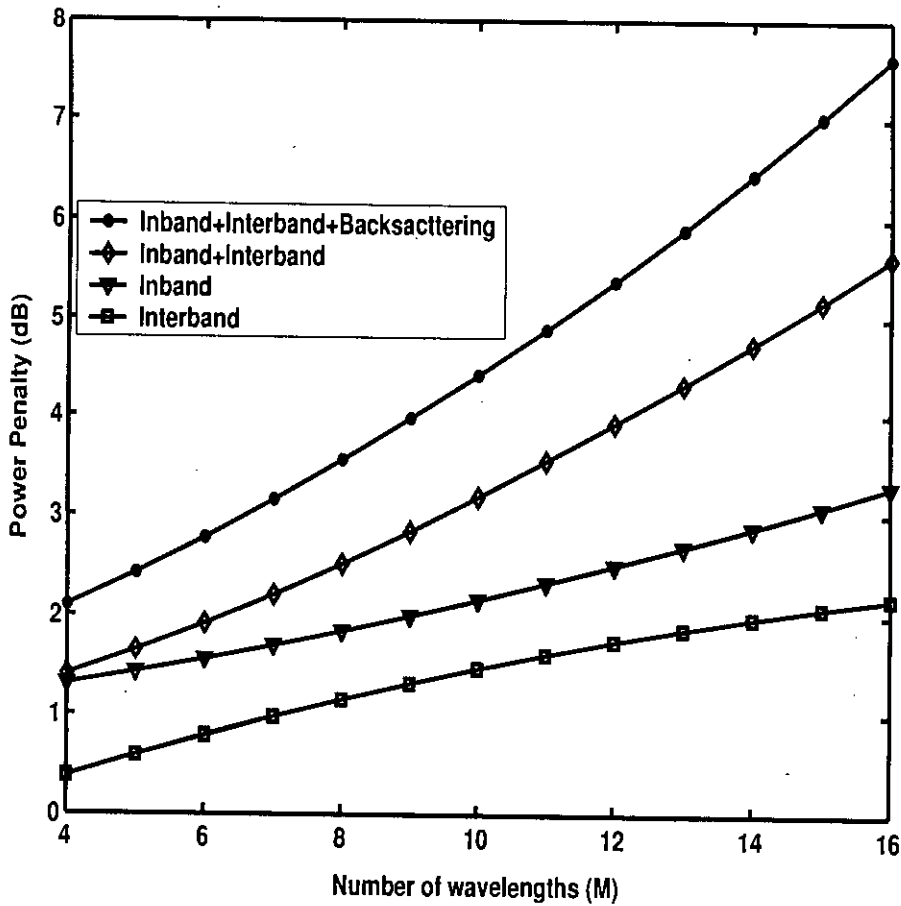
Figure 4.9: Power penalty due to different types of crosstalk in unidirectional and bidirectional OXCs against the number of wavelengths. Number of channels, channel separation, backscattering coefficient, and component crosstalk are kept fixed in this regard. Power penalty is plotted for an overall BER of 10^{-9}. N = 8, $\Delta\lambda$=0.006nm, $R_{bs} = -25$ dB, and $R_c = -40$ dB.

Figure 4.8 gives the plot of BER performance due to all kinds of crosstalk present in an OXC of a WDM system. To observe the relative effect of different kinds of crosstalk on the performance of BER, impact of all kinds of crosstalk on BER performance are depicted in the same plot. From the plot of Figure 4.8, it is clear that inter-band crosstalk causes the lowest BER. The effect of in-band crosstalk is found to be more vulnerable than the inter-band crosstalk in this analysis. The topmost curve shows the BER performance for the composite effect of in-band, inter-band and backscattering induced crosstalk of a BOXC. Table 4.6 gives the relative BER performance due to different types of crosstalk present in an OXC.

Table 4.6: BER performance due to different types of crosstalk.

Other Parameters	Pr (dBm)	Type of Crosstalk	BER
N = 4, M = 4, R_{bs} = − 25 dB, R_c = − 40 dB, $\Delta\lambda$ = 0.006 nm	− 20	No crosstalk	10^{-17}
		Inter-band	10^{-14}
		In-band	10^{-13}
		In-band + inter-band	10^{-12}
		In-band + inter-band + backscattering	10^{-9}

Figure 4.9 depicts the plot of power penalty against the number of wavelengths per channel for all kinds of crosstalk. This power penalty is plotted to achieve a standard BER of 10^{-9}. It gives the relative scenario of power penalty caused by different types of crosstalk due to OXC in a WDM system. From the plot, we see that inter-band crosstalk causes the least power penalty and power penalty caused by BOXC with the composite effect of in-band, inter-band and backscattering induced crosstalk is maximum. Table 4.7 gives the relative values of power penalty due to different types of crosstalk that is present in an OXC.

The BER performance due to the composite effect of in-band, inter-band and backscattering induced crosstalk in a BOXC of a WDM system is plotted in Figure 4.10 [(a)-(b)] for varying number of wavelengths per channel. These plots also show the effect of variation of number of input channels on the BER performance. It is found from the simulation that for a fixed number of channels, the BER increases with the increase of number of wavelengths per channel. The BER also increases with the increase in number of channels for a fixed number of wavelengths per channel. So, for some other fixed system parameters, the number of channels or the number of wavelengths per channel are limited by the effect of crosstalk.

Table 4.7: Power penalty due to different types of crosstalk.

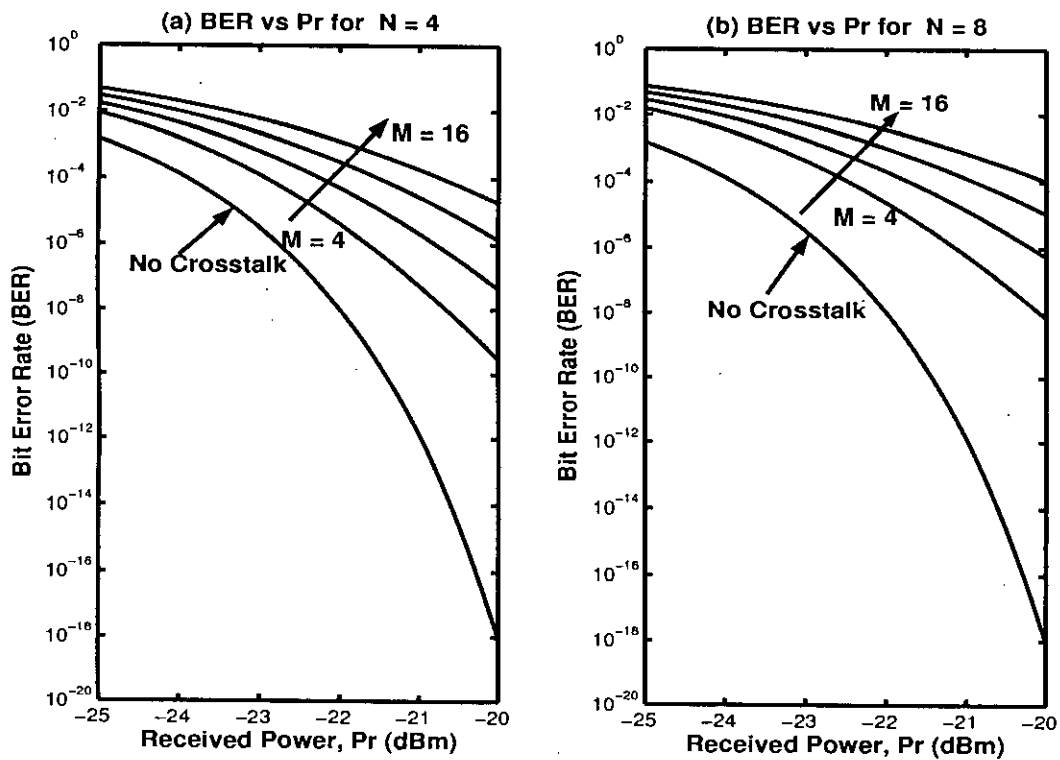| M	Type of Crosstalk	PP (dB)
12	Inter-band	1.8
	In-band	2.4
	In-band + inter-band	4.0
	In-band + inter-band + backscattering	5.4

Figure 4.10: BER performance of BOXCs with the variation of number of wavelengths and number of channels. Backscattering coefficient, component crosstalk, and channel separation are kept fixed in this condition. $R_{bs} = -25$ dB, $R_c = -40$ dB, and $\Delta\lambda=0.006$nm.
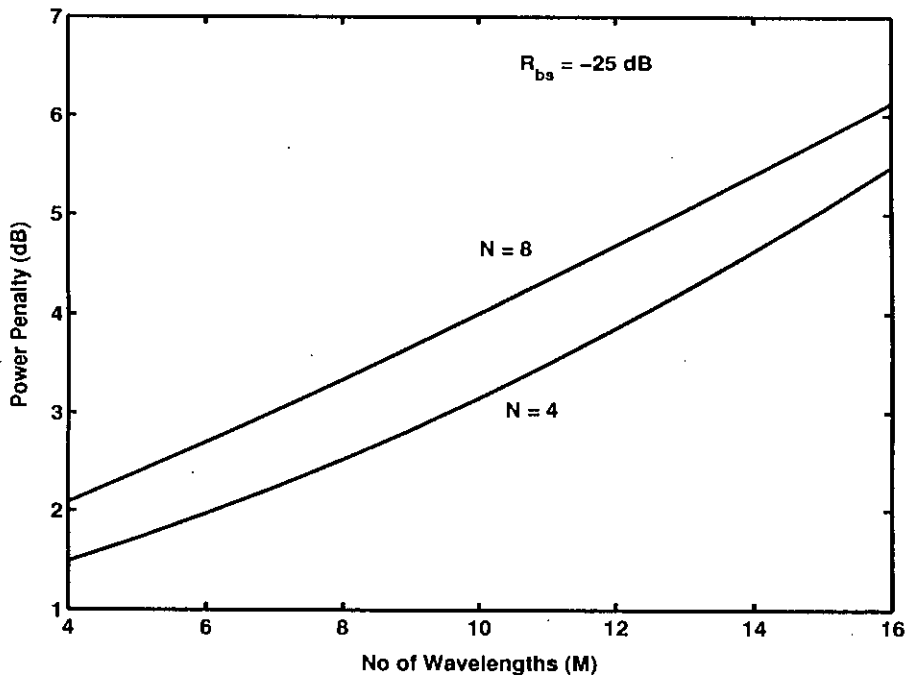
Figure 4.11: Dependance of power penalty on the number of wavelengths and number of input fibers of BOXCs. Backscattering coefficient, component crosstalk, and channel separation are considered to be fixed. $R_{bs} = -25$ dB, $R_c = -40$ dB, and $\Delta\lambda=0.006$nm. Power penalty is plotted to get an overall BER of 10^{-9} from the plot of Figure 4.10.

In Figure 4.11, power penalty due to the composite effect of in-band, inter-band and backscattering induced crosstalk in a BOXC is plotted against the number of wavelengths per channel. This power penalty is also plotted for a standard BER of 10^{-9}. Relative effect of number of channels on power penalty for a fixed number of wavelengths per channel have also been plotted. Increase in number of channels causes an upward shift of power penalty curve signifying that power penalty increases with the increase of number of channels.

As stated earlier, backscattering induced crosstalk is a serious problem in BOXCs. We investigated the effect of variation of backscattering induced noise on BER performance of BOXCs in a WDM system and the simulation results are plotted in Figure 4.12. With the increase of the backscattering coefficient R_{bs}, we get an increase of BER. Comparative analysis is also done by varying the number of
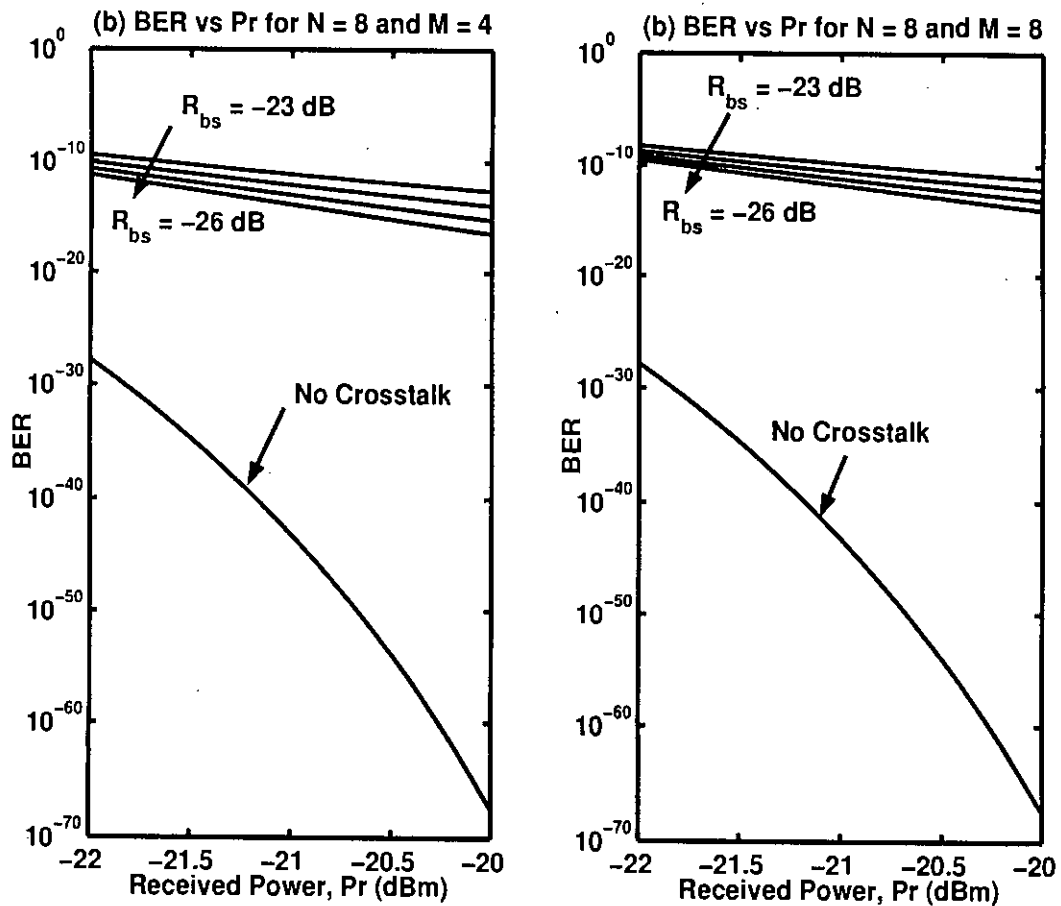
Figure 4.12: BER performance of BOXCs with varying backscattering coefficients and varying number of wavelengths. Component crosstalk and channel separation are considered to be fixed. $R_c = -40$ dB and $\Delta\lambda = 0.006$nm.

wavelengths per channel in each case and we found a significant change in BER with the change of number of wavelegnths per channel. Table 4.8 describes the effect of backscattering induced crosstalk on the BER performance of a WDM system.

Finally, the power penalty of BOXC due to the composite effect of all types of crosstalk is studied against the backscattering coefficient. The result is depicted in Figure 4.13. It is found that the power penalty is very large even for the small number of channels and for the small number of wavelengths per channel. The variation of power penalty with number of wavelengths per channel for a fixed

Table 4.8: BER performance due to backscattering induced crosstalk.

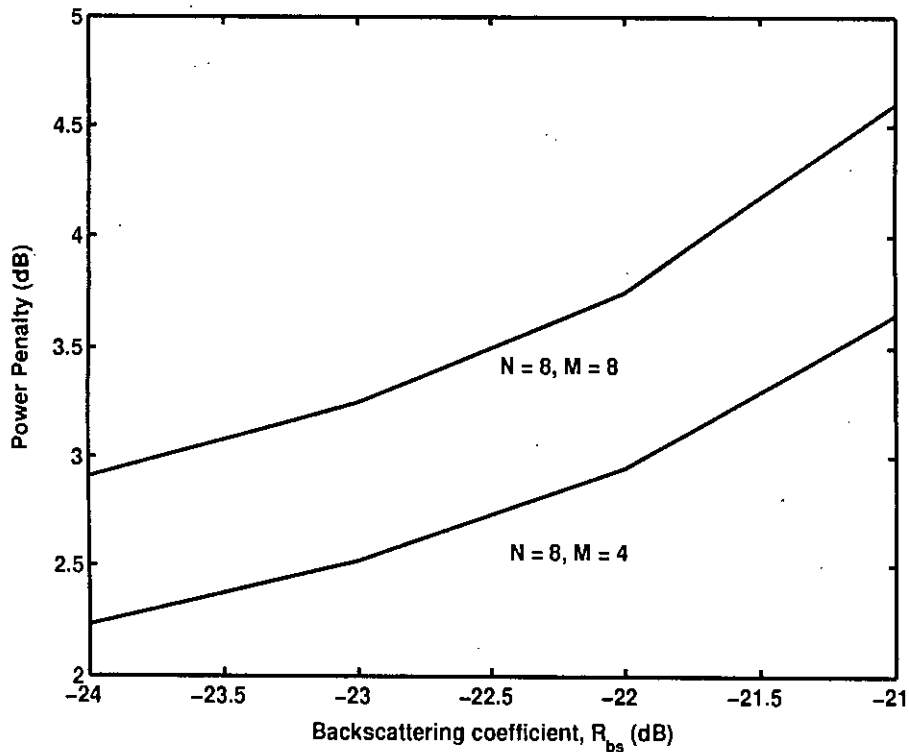| Other Parameters	R_{bs} (dB)	BER
$Pr = -20$ dBm, $R_c = -40$ dB, M = 4, N = 8	-26	10^{-17}
	-23	10^{-13}

Figure 4.13: Dependance of power penalty on the backscattering coefficient R_{bs} for BOXCs. Power penalty is plotted for an overall BER of 10^{-9} and the data is obtained from Figure 4.12. Dependency on number of wavelength is also shown.

backscatering coefficient is also plotted in this figure. Table 4.9 gives the relative values of power penalty with the variation of backscattering coefficient and number of wavelengths per channel.

Table 4.9: Power penalty due to backscattering induced crosstalk.

N	R_{bs} (dB)	M	PP (dB)
8	− 23	4	2.5
		8	3.25
	− 21	4	3.6
		8	4.6

4.4   Summary

Detail simulation is done in this chapter considering the effect of in-band, inter-band and backscattering induced crosstalk on BER performance and power penalty due to unidirectional and bidirectional OXCs in a WDM network. This simulation is done based on the analytical expression developed in section 3.7. The comparative effect of different system parameters on BER performance and power penalty is also discussed in this chapter.

Chapter 5

Conclusion and Scope of Future Work

5.1 Conclusion

The effect of in-band and inter-band crosstalks are considered together for uni-directional multiwavelength OXC. The effect of backscattering induced crosstalk due to BOXC in bidirectional WDM system is also realized. The analytical expression of BER due to in-band crosstalk in multiwavelength OXC is developed based on the study of single wavelength OXC [6]. Many literatures identified the presence of inter-band crosstalk but ultimately ignored as this crosstalk can be removed by the well-designed receiver filter. In our study, it is identified that the inter-band crosstalk due to the frequency characteristics of received digital bit patterns can not be eliminated by receiver filters. This crosstalk can be severe when the channel separation becomes very small. An analytical expression for this inter-band crosstalk is developed in our study. A bidirectional model of a WDM system is given in this study and the expression of BER is modified considering in-band, inter-band and backscattering induced crosstalk. Necessary simulation has been done regarding the calculation of BER and power penalty with different varying system parameters for unidirectional and bidirectional optical fiber communication. This study enables us to do compromise between different system parameters to achieve a particular network performance.

The effect of in-band crosstalk on BER performance is investigated. It is found that BER due to in-band crosstalk increases with the increase of number of channels . For N=4, M=8, BER = 10^{-13} , and for N = 12, M=8, BER = 10^{-9}. It is also found that the BER increases with the increase of number of wavelengths per channel due to in-band crosstalk. For N = 12, M=8, BER = 10^{-9} and for N=12, M=12, BER = 10^{-8}. BER also increases with the increase of component crosstalk due to in-band crosstalk. For N=4, M=8, Rc = -45 dB, BER = 10^{-15} and for N=4, M=8, Rc= -40 dB BER = 10^{-13}.

From the findings of BER performance due to in-band crosstalk, power penalty is calculated. It is found that power penalty due to in-band crosstalk increases with the increase of number of channels. For N=4, M=12, Rc=-40dB, PP = 2 dB and for N=16, M=12,Rc= -40 dB, PP = 4.2 dB. Power penalty also increases with the increase in number of wavelengths per channel. For N=4, M=8,Rc= -40 dB, PP = 1.3 dB and for N=4, M=12, Rc=-40dB, PP = 2 dB. It is also found that power penalty due to in-band crosstalk also decreases with the decrease in component crosstalk. For N=4, M=12, Rc=-40dB, PP = 2 dB and for N=4, M=8, Rc=-45dB, PP = 1.21 dB.

The effect of inter-band crosstalk on network performance is studied. It is found that the inter-band crosstalk increases with the increase of number of wavelengths. For M=8, Crosstalk=-85.5 dBm and for M=16, Crosstalk=-83 dBm for some other fixed system parameters. It is also found that inter-band crosstalk decreases with the increase in channel separation. For M=8, $\Delta\lambda = 0.02$ nm, Crosstalk = -85.5 dBm and for M=8, $\Delta\lambda = 0.1$ nm, Crosstalk = - 106 dBm.

The effect of inter-band crosstalk on BER performance is studied and it is found that BER increases with the increase in number of wavelengths. For M=8, $\Delta\lambda = 0.004$ nm, BER = 10^{-14} and for M=16, $\Delta\lambda = 0.004$ nm, BER = 10^{-9}. It is also found that BER decreases with the increase in channel separation. For M=8, $\Delta\lambda = 0.004$ nm, BER = 10^{-14} and for M=8, $\Delta\lambda = 0.01$ nm, BER = 10^{-15}.

The effect of inter-band crosstalk on power penalty is also studied. It is found that power penalty increases with the increase in number of wavelengths. For

M=16, $\Delta\lambda = 0.004$ nm, PP = 1.9dB and for M=32, $\Delta\lambda = 0.004$ nm, PP = 4.2dB. It is also found that power penalty due to inter-band crosstalk increases with the decrease in channel separation. For M=16, $\Delta\lambda = 0.01$ nm, PP = 0.57dB and for M=16, $\Delta\lambda = 0.004$ nm, PP = 1.9dB.

Finally, the effect of backscattering in bidirectional communication is studied. It is found that the effect of backscattering increases the BER. For some fixed system parameters,without backscattering, the BER= 10^{-12} and with backscattering the BER= 10^{-9}. It is also found that the effect of backscattering increases the power penalty. Without backscattering PP=4.0 dB and with backscattering PP=5.4 dB for some other fixed system parameters. It is also found that with the increase of backscattering coefficient BER increases. For Rbs=-26 dB, BER = 10^{-17} and for Rbs=-23 dB, BER = 10^{-13}. From the BER performance it is calculated that the power penalty also increases with the increase of backscattering coefficient. For M=8, Rbs=-23 dB, PP=3.25 dB and for M=8, Rbs=-21 dB, PP=4.6 dB.

5.2   Scope of Future Work

In our work, nonlinear crosstalk, amplifier crosstalk, receiver noise other than the thermal noise are not considered. Again, coherent and incoherent crosstalk are not considered separately. So, future work can be done considering all the above factors in the expression of BER to observe the network performance.

Bibliography

[1] Hill, G.R. et al., "A transport network layer based on optical network element," *J. Lightwave Technol.*, vol. 11, no. 5/6, pp. 667- 679, May/June 1993.

[2] Iannone, E. and Sabella, R., "Optical path technologies: A comparison among different cross-connect architectures," *J. Lightwave Technol.*, vol. 14, no. 10, pp. 2184 - 2194, Oct. 1996.

[3] Okamoto, S., Watanabe, A. and Sato, K., "Optical path cross-connect node architectures for photonic transport network," *J. Lightwave Technol.*, vol. 14, no. 6, pp. 1410 - 1422, June 1996.

[4] Zhou, J. et al., "Crosstalk in multiwavelength optical cross-connect networks," *J. Lightwave Technol.*, vol. 14, no. 6, pp. 1423 - 1435, June 1996. *J. Lightwave Technol.*, vol. 14, no. 6, pp. 1410 - 1422, June 1996.

[5] Gyselings, T., Morthier, G. and Baets, R., "Crosstalk analysis of multiwavelength optical cross connects," *J. Lightwave Technol.*, vol. 17, no. 8, pp. 1273 - 1283, Aug 1999.

[6] Takahashi, H., Oda, K. and Toba, H., "Impact of crosstalk in an arrayed waveguide multiplexer on NN optical interconnection," *J. Lightwave Technol.*, vol. 14, no. 6, pp. 1120 - 1126, June 1996.

[7] Dods, S. D., Lacey, J. P. R. and Tucker, R. S.,"Homodyne crosstalk in WDM ring and bus networks," *IEEE photon. Technol. Lett.*, vol. 10, no. 3, pp. 457 - 458, Mar. 1998.

[8] Ho, K.P., Chan, C. K., Tong, F. and Chen, L. K., "Exact analysis of homodyne crosstalk induced penalty in WDM networks," *IEEE photon. Technol. Lett.,* vol. 9, no. 3, pp. 1285 - 1287, Sept. 1997.

[9] Dods, S. D., Lacey, J. P. R. and Tucker, "Performance of WDM ring and bus network in the presence of homodyne crosstalk," *J. Lightwave Technol.,* vol. 17, no. 3, pp. 388 - 396, Mar. 1999.

[10] Shen, Y., Lu, K. and Gu, W., "Coherent and incoherent crosstalk in WDM optical networks," *J. Lightwave Technol.,* vol. 17, no. 5, pp. 759 - 764, May 1999.

[11] Kim, C. H., Lee, C. H. and Chung, Y. C., "Bidirectional WDM self-healing ring network on simple bidirecional add/drop amplifier modules," *IEEE photon. Technol. Lett.,* vol. 10, no. 9, pp. 1340 - 1342, Sept. 1998.

[12] Simmons, J. M. and Saleh A. A. M. et al., "Optical crossconnects of reduced complexity for WDM ring networks with bidirectional symmetry," *IEEE photon. Technol. Lett.,* vol. 10, no. 6, pp. 819 - 821, June 1998.

[13] Park, S. K and Park, J. W. et al., "Multiwavelength bidirectional optical crossconnects using fiber bragg grating and polarization beam splitters," *IEEE photon. Technol. Lett.,* vol. 12, no. 7, pp. 888 -890, July 2000.

[14] Kim, J. and Lee, B., "Independently switchable bidirectional optical cross connects," *IEEE photon. Technol. Lett.,* vol. 12, no. 6, pp. 693 - 695, June 2000.

[15] Kim, S., "Bidirectional optical crossconnects for multiwavelength ring networks using single arrayed waveguide grating router," *J. Lightwave Technol.,* vol. 20, no. 2, pp. 188 - 194, Feb. 2002.

[16] Yuan, H., Zhong, W. and Hu, W., "FBG-Based bidirectional optical cross connects for bidirectional WDM ring networks," *J. Lightwave Technol.,* vol. 22, no. 12, pp. 2710 - 2721, Dec. 2004.

[17] Keiser, G., *"Optical Fiber Communication,"* 3rd Edition, McGraw-Hill Companies, Inc., 2000.

[18] Ramaswami, R.,Sivaranjan, K.N, *"Optical Networks,"* 2nd Edition, Morgan Kaufmann Publishers, 2002.

[19] Idelfonso, T.M.,Eduward, T., *"Crosstalk in WDM Communication Networks ,"* The Springer International Series in Engineering and Computer Science , Vol. 678 , 2002.

[20] Pointurier, Y. and Pierce, B. et al., *"Cross-Layer Design of All-Optical Networks Incorporating Crosstalk Effects ,"* Ph.D. thesis, School of Engineering and Applied Science, University of Virginia, 2006.

[21] Cuenot, B., *"Contribution to engineering of WDM $N \times 160$ Gbit/s optical transmission systems. Analysis of optical signal degradation induced by propagation impairments."* Ph.D. thesis, The Louis Pasteur University of Strasbourg, 2004.

[22] Agrawal, G. P., *"Nonlinear Fiber Optics ,"* 3rd Edition, Academic Press, San Diego, CA, 2001. The Springer International Series in Engineering and Computer Science , Vol. 678 , 2002.

Index